## **Ceramics International**

# Presence of K+ in solution acts as a protectant against dissolution of biomimetic apatites compared to Na+ --Manuscript Draft--

Manuscript Number:	CERI-D-23-11935R1
Article Type:	Full length article
Keywords:	B Spectroscopy; C Chemical properties; D Apatite; E Biomedical Applications; B Impurities
Corresponding Author:	Alix Deymier UCONN HEALTH CENTER Farmington, CT UNITED STATES
First Author:	Stephanie Wong
Order of Authors:	Stephanie Wong
	Katherine R. Peccerillo
	Margaret Easson
	Trey Doktorski
	Alix C. Deymier
Abstract:	Tooth mineral is constantly exposed to saliva. Based on many factors including diet and chronic disease, salivary composition can vary in pH and potassium (K+) and sodium (Na+) concentrations. Tooth mineral is composed of bioapatite with an ability for ionic exchange between the mineral and the surrounding fluid. Na+ and K+ are known to integrate into biomimetic apatites during crystallization and affect crystallization growth/rate and morphology of calcium phosphates. However, it is unknown how exogenous Na+ and K+ in the solution affect carbonated apatite after formation. Therefore, we investigated the mechanistic differences between Na+ and K+ on biomimetic apatite dissolution/recrystallization. To do so, biomimetic carbonated apatites with 3 or 7 wt% CO32- were exposed to NaCl or KCl solutions at various concentrations and pHs seen in saliva. Powder mass, Raman, FTIR, and XRD were used to determine the weight, composition, and structure of the mineral while the solution was characterized for pH and ionic variations. After mineral-solution exposure, significant differences were seen between NaCl and KCl solutions. The apatites exposed to NaCl underwent a classical dissolution/recrystallization mechanism exhibiting more loss in mass and carbonate during dissolution with modifications of A-, B-, and labile CO32- amounts during recrystallization which were dependent on the initial apatite CO32- content. Meanwhile, apatites exposed to KCl had less mass loss during dissolution and retained the crystal structure, A-, B-, and labile CO32- amounts during recrystallization, suggesting that K+ may shield apatites from dissolution. To our knowledge, this is the first study to parse out mechanistic differences between Na+ and K+ on biomimetic carbonated apatite dissolution/recrystallization. Overall, this study will provide insight on how fluctuating Na+ and K+ in saliva may affect tooth mineral composition and structure.



Jan 30<sup>th</sup>, 2024

Dear Editors,

Attached is our updated manuscript now entitled "Presence of K+ in solution acts as a protectant against dissolution of biomimetic apatites compared to Na+" along with our response to reviewers to be considered as a peer reviewed article in *Ceramics International*. Several changes have been made to the manuscript in response to reviewer comments. We believe the paper is greatly improved.

We believe that this study focusing on the relationship between compositional, molecular, and structural properties of apatites in response to varying cationic concentrations in solution falls within the aims of the journal and will be of significant interest to your audience. We are hopeful that it will attract researchers in (bio)mineralization, biomedical engineers with interest in mineralized scaffolds, chemists with interest in environmental remediation, and apatite geologists.

All authors listed have no conflict of interest, financial or otherwise. All authors confirm that this manuscript has not been previously published and is not under consideration by any other journal currently. In addition, the authors have approved the contents of this paper and have agreed to the *Ceramics International* submission policies.

Sincerely,

Stephanie Wong

Down

Dr. Alix Deymier

Corresponding author's mailing address:

Dr. Alix Deymier
Dept. of Biomedical Engineering
School of Dental Medicine
UConn Health
263 Farmington Ave
Mail Code: 1721

Farmington, CT 06030, USA

#### **Response to Reviewers:**

Reviewer #1: The paper titled "Presence of solution K+ acts as a protectant against dissolution of biomimetic apatites compared to Na+" was presented to me for review. I have reviewed the articles and have few concerns before the editor considers it for publishing. Below are my concerns and queries:

#### 1. The title is not descriptive. You should be writing K+ solution or Na+ solution.

Thank you for your review of our manuscript. We appreciate your efforts in making our title clearer. In efforts to keep the title concise, we have changed our title to "Presence of  $K^+$  in solution acts as a protectant against dissolution of biomimetic apatites compared to  $Na^+$ ."

#### 2. In abstract I would prefer authors mention bioapatite as hydroxyapatite

We understand the importance of describing the mineral as accurately as possible. However, biological tooth minerals have been shown to be compositionally and structurally different than hydroxyapatite. It has recently been proven that biological bone and tooth mineral have substantially lower amounts of hydroxylation and are less ordered than hydroxyapatite [1]. Additionally, many studies have identified the true composition of tooth mineral which includes HPO<sub>4</sub><sup>2-</sup> ions, CO<sub>3</sub><sup>2-</sup> ions, and other substitutions [2–5]. While the crystal structure is similar to hydroxyapatite, there are other structural differences in biological mineral, such as the hydrated amorphous layer. Additionally, bioapatite is much less crystalline compared to hydroxyapatite, which our synthesis methods reflect [21]. Identifying the mineral used in this study as hydroxyapatite implies that it may be stoichiometric and may be closer to geological apatite, which is not the case. Synthesizing hydroxyapatite is a different method than the synthesis used here as well. In addition, our XRD patterns resemble biological apatite instead of hydroxyapatite. Therefore, we believe that describing the mineral as bioapatite is more accurate than hydroxyapatite.

## 3. Whether Na and K have effect on carbonated apatites, there is not enough justification provided.

We respectfully disagree with this comment. This study repeated shows that there are very significant differences in the ways apatite react in K<sup>+</sup> containing solutions versus Na<sup>+</sup> containing solutions. These include (1) a significant variation in the buffering of the solution as seen by the change in solution pH (2) a reduction in the amount of mineral mass lsot with exposure to KCl as compared to NaCl (3) significant variations in the type of CO<sub>3</sub> affected by solution exposure (4) as well as strucutral differences. These have all been shown to be statistically significant. Further statistical details can be seen in our supplemental tables.

4. Introduction is weak, and I think its better the authors provide some justification of the validity of the concentrations used for Na and K.

We appreciate the concern for the introduction. We have included several edits to our introduction to make it more robust.

To address the concerns about the concentrations: we chose the concentrations in this study based on the Na and K concentrations seen in saliva as described in previous literature [22-28]. This is mentioned in the first paragraph of the introduction. It is also mentioned within the methods section that the concentrations and pHs "represent low and high amounts of Na<sup>+</sup> or K<sup>+</sup> concentrations at acidic and neutral pH's that can occur in the mouth [6,7]." To provide further clarifications, we have added the following blue section within the last paragraph of the introduction: "Therefore, the goal of this study was to determine how extant biomimetic carbonated apatite is altered during exposure to Na<sup>+</sup> and K<sup>+</sup>-rich solutions that simulate the concentrations range of Na<sup>+</sup> and K<sup>+</sup> within saliva."

## 5. Is tooth mineral reaction during salivary variations in Na+ or K+ content a decisive role? Can the authors comment more on its importance.

Tooth mineral is known to undergo dissolution and recrystallization constantly. It is also known that apatites can be readily substituted with Na<sup>+</sup> and K<sup>+</sup>. If there is constantly high concentrations of Na or K within the saliva, this suggests that Na<sup>+</sup> and K<sup>+</sup> may substitute within the tooth mineral. Our lab has previously found that Na<sup>+</sup> and K<sup>+</sup> co-substitutions with CO<sub>3</sub><sup>2-</sup> within the lattice can alter the amount of B-type and A-type CO<sub>3</sub><sup>2-</sup> substitutions as well as the physiochemical and crystal structure properties. This suggests that this may happen within our tooth mineral. Our unpublished data also shows that the mechanics of these minerals with increasing amounts of K<sup>+</sup> or Na<sup>+</sup> substitutions are different at higher cosubstitutions of wt% CO<sub>3</sub><sup>2-</sup> in which K<sup>+</sup> maintains the bulk modulus of highly carbonated apatites similar to lowly carbonated apatites. At the same wt% CO<sub>3</sub><sup>2-</sup>, Na<sup>+</sup> exhibits a substantial decrease in the bulk modulus compared to lower wt% CO<sub>3</sub><sup>2</sup>. The increasing addition of Na<sup>+</sup> or K<sup>+</sup> into biomimetic apatites implies that the tooth composition, structure, and mechanics may be varied with Na<sup>+</sup> and K<sup>+</sup> substitutions. As this was different amounts of Na<sup>+</sup> and K<sup>+</sup> within the crystal structure, this also suggests that fluctuations Na<sup>+</sup> and K<sup>+</sup> in the solution outside of the apatite may also affect the composition, structure, and mechanics of biological apatite, especially tooth mineral in which the salivary composition is known to change.

In terms of bone, past literature has shown that high sodium is associated with osteoporosis [8]. On the other hand, high potassium diets exhibit the opposite where it is associated with higher bone mineral density [9]. While this was not initially in mind when this study was materializing, the study here follows trends with what is seen clinically in bone. Therefore, this may begin to describe what may occur within bone as well.

## 6. Tooth mineral is very general. Authors need to be specific which tooth minerals they are concerned about or addressing to.

Thank you for this comment. We have included "enamel and dentin" throughout the introduction to specify the tooth mineral we are concerned about. Our XRD patterns of the 3 and 7 wt% CO<sub>3</sub><sup>2-</sup> resemble these tissues, especially for enamel (Supplemental Figure 7).

#### 7. There should be a paragraph about the description of the methodologies.

It is unclear as to what the description of the methodologies should be as we have provided our methods and a visual representation of our dissolution experiment within the Methods section and Supplemental Figure 1.

## 8. In Methods (Synthesis) part, please mention the country for Sigma Aldrich. In fact in all sections where mentioned.

Thank you for this comment as this will provide clarity on where the chemicals are from. We have added the country of origin for all chemicals within the manuscript and it is highlighted in yellow.

#### 9. "Once completely titrated, the mixture was digested for 2 hours". Explain.

The precipitated crystals within the synthesis solution were left alone at 60°C at ~pH 9 to mature during the 2 hours to obtain more crystalline apatite. We understand that the sentence in the manuscript may not be clear, thus, this sentence now reads in the revised manuscript as:

"Once completely titrated, the mixture was left to mature for 2 hours at ~pH 9 at 60°C."

- 10. For the Raman spectroscopy methodology, many things are missing. The macrophage polarization states were evaluated using Raman spectroscopy. The evaluation performed for each Raman band observed was done based on published literature? If yes, can you mention it. Did these spectrums represent the mean of 100 independent recordings obtained from the apatite subsets in each specimen showing any significant changes? This information needs to be provided. Why did the authors did not do a principal component analysis of the Raman data between the groups? Because the scores will be indicative of the dispersion of samples within orthogonal directions.
  - I normally create a final spectrum by combining the number of images and performing baseline correction using a fifth-degree polynomial function. Did you?

In this study, we looked at the dissolution and recrystallization of biomimetic apatites without cells. The manuscript does not mention macrophages or differentiation of any cells. The analysis of the carbonate to phosphate ratio of the mineral powders was determined via Raman by calculating the peak area of the  $v_1 CO_3^{2-}$  at  $1070 \text{ cm}^{-1}$ ,  $v_1 PO_4^{3-}$  at  $950 \text{ cm}^{-1}$ , and  $v_1 PO_4^{3-}$  at  $960 \text{ cm}^{-1}$ . This was obtained via peak deconvolution for each of the 10 individual recordings for each replicate where each condition had 3 replicates as described within the Raman methodology. The  $CO_3/PO_4$  ratio and the peak assignments have been extensively determined and used within the literature for synthetic apatites as well as bone and teeth samples [10–14]. We have also added several of these citations into the Raman methods section, which are highlighted within the revised manuscript.

Thank you for the suggestion to do a principal component analysis. Although PCA could allow us to more clearly differentiate between the groups, it is not a easy task to interpret those principal components. By choosing to look at specific factors, we are able not

only to see differences between groups but to establish clearly what those differences are and how they relate to each other based on the literature. Thanks to this we are able to suggest mechanisms for the observed behaviors and not just identify differing populations.

We included a representative spectrum of the 3 and 7 wt% CO<sub>3</sub><sup>2-</sup> before exposure in the newly added Supplemental Figure 6.

#### 11. What software did you use for Raman?

We used the WiTec Program 5.1 software for the analysis of the carbonate to phosphate ratio as mentioned under the Raman Spectroscopy methods.

#### 12. X ray diffraction is well written.

We appreciate this comment.

13. The standard and average values of biological apatite described in textbooks do not apply to actual subjects, and reported analytical values differ among researchers. So there is always confusion. To prevent further confusion, it is necessary to correctly understand the term apatite across disciplinary boundaries and clearly define it when using it. Recently, biological apatite has been confused with carbonate apatite, so it is necessary to recognize that carbonate apatite and carbonated hydroxyapatite produced by biological organisms are quite different.

While it is well recognized that it is difficult to obtain human biological samples, there are plenty of articles that have bone, enamel, and dentin samples from human tissue, which have been well characterized. Bone and tooth mineral have been shown to have substantially less hydroxylation compared to synthetic and geological hydroxy(1)apatite [1,15]. In this study, the apatites made were OH deficient obtained through the synthesis methods described in the text. This is shown by the lack of the OH peak at ~3500 cm<sup>-1</sup> and the small OH shoulder at ~630 cm<sup>-1</sup> in the v<sub>4</sub> PO<sub>4</sub><sup>3-</sup> region in the FTIR (Supplemental Figure 5). In addition, these biomimetic apatites have A-type CO<sub>3</sub><sup>2</sup>-, in which this CO<sub>3</sub><sup>2</sup>- substitutes for the OH groups (Figure 3A). This provides even less OH groups in our apatite system. In addition, these synthesis methods were adapted from previous literature [16], in which the XRD pattern and FTIR spectrum resembles biological apatite (Supplemental Figure 5 and Supplemental Figure 7) [2–4,17,18]. These apatites have other substitutions – such as HPO<sub>4</sub><sup>2</sup>as indicated by the right shoulder of the  $v_4 PO_4^{3-}$  peak (~550-530 cm<sup>-1</sup>) – that are not within pure hydroxyapatite. Therefore, it is not accurate in describing these biomimetic apatites as hydroxy(1)apatite and, thus, carbonated hydroxyapatite. Carbonate apatite has been widely referred to as the general composition for biological minerals and is generally accepted within the mineralogical/geological fields as well [1,18–20]. It is important to note that carbonated apatite can be synthesized through various methods and confirming the XRD pattern and FTIR spectrum are biomimetically relevant should be achieved if comparing to bone and tooth mineral.

14. Please put in some limitations related to the number of samples used.

We appreciate this valid concern. We have added this to the limitations section of the discussion. This is written within the manuscript as:

"Furthermore, the conditions shown here were performed in triplicate. While the standard deviations were relatively small for most of the dependent factors, more replicates would be needed in future studies to further determine the statistical power."

#### Reviewer #2:

The manuscript "Presence of solution K+ acts as a protectant against dissolution of biomimetic apatites compared to Na+" is an interesting work. The authors present many results on the exposure of carbonated apatites (2 different CO3 contents) in NaCl and KCl solutions with 3 concentrations at 2 different pH and also at neutral pH, and the changes in pH were taken at different times. The manuscript is well done but difficult to follow due to the number of the hard data results. Due to the relevance of the study, it is desirable that each aspect of the research be described clearly and concisely regarding the effect of the variables described above on the dissolution/precipitation mechanism and the mechanics mentioned in the abstract of the manuscript. Additionally, there are comments and questions that need to be resolved before being considered for publication in Ceramics International.

1. Divide your article into clearly defined and numbered sections (see Guide for Authors of Ceramics International)

Thank you for catching this. We have numbered the sections accordingly.

#### 2. Abstract

2.1 Page 3, lines 14-15 ... "Therefore, we investigated the mechanistic differences between Na+ and K+ on biomimetic apatite dissolution/recrystallization." ... What means "...the mechanistic differences...."? no mechanism on biomimetic apatite dissolution/recrystallization is proposed along the text to mark differences between Na+ and K+.

We have edited the abstract to clarify the dissolution/recrystallization aspect. With the highlighted edits, the section now reads as:

"The apatites exposed to NaCl underwent a classical dissolution/recrystallization mechanism exhibiting more loss in mass and carbonate during dissolution with modifications of A-, B-, and labile  $CO_3^{2-}$  amounts during recrystallization which were dependent on the initial apatite  $CO_3^{2-}$  content. Meanwhile, apatites exposed to KCl had less mass loss during dissolution and retained the crystal structure, A-, B-, and labile  $CO_3^{2-}$  amounts during recrystallization, suggesting that K<sup>+</sup> may shield apatites from dissolution.

## 2.2 Page 3 line 32 "...and mechanics."

No results regarding mechanics are presented in the manuscript.

Thank you for this comment. We have taken this out of the abstract to clarify the intent of our study.

#### 3. Synthesis

Page 5 lines 22-25 ... "The amount of carbonate was determined by comparing the carbonate to phosphate ratio to our standardized carbonate apatites made using a similar precipitation synthesis."... This phrase needs reference. How were these apatites standardized to be used as a reference?

We appreciate this comment as this will help clarify the standardization for others. The carbon content was determined via Carbon Hydrogen Nitrogen analysis for a separate suite of synthetic apatites with increasing  $CO_3^{2-}$  content created in a similar fashion as described in this study. The carbon content for the apatites was assumed to be  $CO_3^{2-}$ . Raman spectroscopy was then used on the same suite of carbonated apatite to analyze the carbonate to phosphate ratio  $(CO_3/PO_4)$  as indicated by section 2.3 Raman Spectroscopy methods. A linear correlation between the  $CO_3/PO_4$  and  $CO_3^{2-}$  was determined and the linear equation was used to determine the amount of carbonate in the apatites here in this study.

The following edits in yellow were added to the synthesis section:

"The amount of carbonate was determined by comparing the carbonate to phosphate ratio to our standardized carbonate apatites that were correlated to the carbon amount determined by Carbon Hydrogen Nitrogen [16]."

#### 4. Results

4.1 It is desirable that each aspect of the research be described clearly and concisely regarding the effect of the variables described above on the dissolution/precipitation mechanism and the mechanics mentioned in the abstract of the manuscript.

As mentioned above, the mechanics has been removed from this study. The mechanics analysis became a much larger undertaking and will be published separately. In the results section we avoid performing any kind of interpretation. We have used this section as a way to lay out the many outcomes of the study but without putting it into context. We have left this interpretation and contextualization for the discussion section.

As mentioned below in response to your comment about the discussion section, we realize that this section had become quite wordy and possibly failed to make clear what is happening in the system. Therefore, many edits and deletions have been made to make it more clear and concise. Due to the interrelated nature of the measures made here (pH affects mass loss which affects carbonate release which affects lattice structure, etc...) it is not possible to isolate the contributions of these many variables when describing their effect on the apatite dissolution-recrystallization. They must be taken into account together to fully understand what is happening. However, we hope that the edits make this complex interpretation more cohesive.

4.2 Figures of the spectra obtained from the FT-IR, Raman analyzes as well as the XRD patterns are necessary to clearly reflect the results shown in the results section or in the supplementary figures section.

Thank you for this comment. We agree that this would make our results more robust. We have added a representative XRD pattern and FTIR and Raman spectra of the unexposed apatites with 3 and 7 wt%  $CO_3^{2-}$ . Please see the newly added Supplemental Figures 5-7.

#### 5. Discussion

A combined results and discussion section is suggested because the discussion of the manuscript repeats many of the results already described in that section and furthermore the discussion of the results is not clear. The discussion of the results should explore the significance of the results of the work, not repeat them.

Thank you for feedback on the discussion. We have made many revisions to the discussion in order to minimize repetition of the results. Although, it is necessary to bring up the results in the discussion section in order to draw correlations between them, these edits should enhance the flow and avoid the feeling of repeated information. Modifications to the discussion are highlighted in yellow. We have not left markers for all of the text that was deleted for easy of reading.

#### References

- [1] B. Wopenka, J.D. Pasteris, A mineralogical perspective on the apatite in bone, Materials Science and Engineering: C 25 (2005) 131–143. https://doi.org/10.1016/j.msec.2005.01.008.
- [2] C. Rey, M. Shimizu, B. Collins, M.J. Glimcher, Resolution-enhanced Fourier transform infrared spectroscopy study of the environment of phosphate ions in the early deposits of a solid phase of calcium-phosphate in bone and enamel, and their evolution with age. I: Investigations in the upsilon 4 PO4 domain, Calcif Tissue Int 46 (1990) 384–394. https://doi.org/10.1007/BF02554969.
- [3] C. Rey, B. Collins, T. Goehl, I.R. Dickson, M.J. Glimcher, The carbonate environment in bone mineral: a resolution-enhanced Fourier Transform Infrared Spectroscopy Study, Calcif Tissue Int 45 (1989) 157–164. https://doi.org/10.1007/BF02556059.
- [4] C. Rey, V. Renugopalakrishman, B. Collins, M.J. Glimcher, Fourier transform infrared spectroscopic study of the carbonate ions in bone mineral during aging, Calcif Tissue Int 49 (1991) 251–258. https://doi.org/10.1007/BF02556214.
- [5] S. Von Euw, Y. Wang, G. Laurent, C. Drouet, F. Babonneau, N. Nassif, T. Azaïs, Bone mineral: new insights into its chemical composition, Scientific Reports 9 (2019) 1–11. https://doi.org/10.1038/s41598-019-44620-6.
- [6] M. Crisostomo, C. Ureta, Salivary pH and Taste Sensitivity among Geriatric and Non-Geriatric Patients in a Tertiary Hospital: A Cross Sectional Study, Philippine Journal of Otolaryngology Head and Neck Surgery 34 (2019) 11–15. https://doi.org/10.32412/pjohns.v34i2.125.
- [7] M.J. Larsen, A.F. Jensen, D.M. Madsen, E.I.F. Pearce, Individual variations of pH, buffer capacity, and concentrations of calcium and phosphate in unstimulated whole saliva, Archives of Oral Biology 44 (1999) 111–117. https://doi.org/10.1016/S0003-9969(98)00108-3.
- [8] S. Hong, J.W. Choi, J.-S. Park, C.H. Lee, The association between dietary sodium intake and osteoporosis, Sci Rep 12 (2022) 14594. https://doi.org/10.1038/s41598-022-18830-4.
- [9] J. Ha, S.-A. Kim, K. Lim, S. Shin, The association of potassium intake with bone mineral density and the prevalence of osteoporosis among older Korean adults, Nutr Res Pract 14 (2020) 55–61. https://doi.org/10.4162/nrp.2020.14.1.55.
- [10] A.L. Boskey, Bone composition: relationship to bone fragility and antiosteoporotic drug effects, BoneKEy Reports 2 (2013). https://doi.org/10.1038/bonekey.2013.181.
- [11] and M.C.H. van der M. Eve Donnelly, Adele L. Boskey, Shefford P. Baker, Effects of tissue age on bone tissue material composition and nanomechanical properties in the rat cortex, Journal of Biomedical Materials Research Part A 92 (2010) 1048–1056. https://doi.org/10.1161/CIRCULATIONAHA.110.956839.
- [12] M.M. Moynahan, S.L. Wong, A.C. Deymier, Beyond dissolution: Xerostomia rinses affect composition and structure of biomimetic dental mineral in vitro, PLoS ONE 16 (2021) 5–7. https://doi.org/10.1371/journal.pone.0250822.
- [13] M. Wang, R. Qian, M. Bao, C. Gu, P. Zhu, Raman, FT-IR and XRD study of bovine bone mineral and carbonated apatites with different carbonate levels, Materials Letters 210 (2018) 203–206. https://doi.org/10.1016/j.matlet.2017.09.023.
- [14] P.G. Spizzirri, N.J. Cochrane, S. Prawer, E.C. Reynolds, A Comparative Study of Carbonate Determination in Human Teeth Using Raman Spectroscopy, Caries Research 46 (2012) 353–360. https://doi.org/10.1159/000337398.

- [15] J.D. Pasteris, C.H. Yoder, M.P. Sternlieb, S. Liu, Effect of carbonate incorporation on the hydroxyl content of hydroxylapatite, Mineralogical Magazine 76 (2012) 2741–2759. https://doi.org/10.1180/minmag.2012.076.7.08.
- [16] A.C. Deymier, A.K. Nair, B. Depalle, Z. Qin, K. Arcot, C. Drouet, C.H. Yoder, M.J. Buehler, S. Thomopoulos, G.M. Genin, J.D. Pasteris, Protein-free formation of bone-like apatite: New insights into the key role of carbonation, Biomaterials 127 (2017) 75–88. https://doi.org/10.1016/j.biomaterials.2017.02.029.
- [17] G.E. Tiznado-Orozco, R. García-García, J. Reyes-Gasga, Structural and thermal behaviour of carious and sound powders of human tooth enamel and dentine, J. Phys. D: Appl. Phys. 42 (2009) 235408. https://doi.org/10.1088/0022-3727/42/23/235408.
- [18] Th. Leventouri, A. Antonakos, A. Kyriacou, R. Venturelli, E. Liarokapis, V. Perdikatsis, Crystal Structure Studies of Human Dental Apatite as a Function of Age, International Journal of Biomaterials (2009) 1–6. https://doi.org/10.1155/2009/698547.
- [19] S. Weiner, H.D. Wagner, THE MATERIAL BONE: Structure-Mechanical Function Relations, Annu. Rev. Mater. Sci. 28 (1998) 271–298. https://doi.org/10.1146/annurev.matsci.28.1.271.
- [20] G.S. Ingram, The Role of Carbonate in Dental Mineral, Caries Res 7 (1973) 217–230. https://doi.org/10.1159/000259845.
- [21] M. Grynpas, The crystallinity of bone mineral, Journal of Materials Science 11(9) (1976) 1691-1696.
- [22] G. Singh, E. Iyer, H. Malik, Relative Changes in Salivary Sodium and Potassium in Relation to Exposure to High G Stress, Med J Armed Forces India 50 (1994) 261–265. https://doi.org/10.1016/S0377-1237(17)31082-1.
- [23] N.A. Thorn, I.L. Schwartz, J.H. Thaysen, Effect of Sodium Restriction on Secretion of Sodium and Potassium in Human Parotid Saliva, Journal of Applied Physiology 9 (1956) 477–480. https://doi.org/10.1152/jappl.1956.9.3.477.
- [24] C. Simões, I. Caeiro, L. Carreira, F.C. e Silva, E. Lamy, How Different Snacks Produce a Distinct Effect in Salivary Protein Composition, Molecules 26 (2021) 2403. https://doi.org/10.3390/molecules26092403.
- [25] A. Almståhl, M. Wikström, Electrolytes in stimulated whole saliva in individuals with hyposalivation of different origins, Archives of Oral Biology 48 (2003) 337–344. https://doi.org/10.1016/S0003-9969(02)00200-5.
- [26] C. Labat, S. Thul, J. Pirault, M. Temmar, S.N. Thornton, A. Benetos, M. Bäck, Differential associations for salivary sodium, potassium, calcium, and phosphate levels with carotid intima media thickness, heart rate, and arterial stiffness, Disease Markers 2018 (2018). https://doi.org/10.1155/2018/3152146.
- [27] B. Kallapur, K. Ramalingam, Bastian, A. Mujib, A. Sarkar, S. Sethuraman, Quantitative estimation of sodium, potassium and total protein in saliva of diabetic smokers and nonsmokers: A novel study, J Nat Sci Biol Med 4 (2013) 341–345. https://doi.org/10.4103/0976-9668.117006. [28] T. Dhondup, Q. Qian, Acid-Base and Electrolyte Disorders in Patients with and without Chronic Kidney Disease: An Update, Kidney Diseases 3 (2017) 136–148. https://doi.org/10.1159/000479968.

## Presence of $K^{\scriptscriptstyle +}$ in solution acts as a protectant against dissolution of biomimetic apatites compared to $Na^{\scriptscriptstyle +}$

Authors: Stephanie Wong<sup>1</sup>, Katherine R. Peccerillo<sup>2</sup>, Margaret Easson<sup>3</sup>, Trey Doktorski<sup>3</sup>, Alix C. Deymier<sup>1,3\*</sup>

- 1. Dept of Biomedical Engineering, University of Connecticut Health Center, Farmington, CT
- 2. School of Dental Medicine, University of Connecticut Health Center, Farmington, CT
- 3. Dept of Biomedical Engineering, University of Connecticut, Storrs, CT

## \*Corresponding Author:

Email: deymier@uchc.edu

Alix Deymier
Dept of Biomedical Engineering
School of Dental Medicine
University of Connecticut Health Center
263 Farmington Ave
Farmington, CT 06030
Phone: 1-520-248-1956

## **Abstract**

Tooth mineral is constantly exposed to saliva. Based on many factors including diet and chronic disease, salivary composition can vary in pH and potassium (K<sup>+</sup>) and sodium (Na<sup>+</sup>) concentrations. Tooth mineral is composed of bioapatite with an ability for ionic exchange between the mineral and the surrounding fluid. Na<sup>+</sup> and K<sup>+</sup> are known to integrate into biomimetic apatites during crystallization and affect crystallization growth/rate and morphology of calcium phosphates. However, it is unknown how exogenous Na<sup>+</sup> and K<sup>+</sup> in the solution affect carbonated apatite after formation. Therefore, we investigated the mechanistic differences between Na<sup>+</sup> and K<sup>+</sup> on biomimetic apatite dissolution/recrystallization. To do so, biomimetic carbonated apatites with 3 or 7 wt% CO<sub>3</sub><sup>2</sup> were exposed to NaCl or KCl solutions at various concentrations and pHs seen in saliva. Powder mass, Raman, FTIR, and XRD were used to determine the weight, composition, and structure of the mineral while the solution was characterized for pH and ionic variations. After mineral-solution exposure, significant differences were seen between NaCl and KCl solutions. The apatites exposed to NaCl underwent a classical dissolution/recrystallization mechanism exhibiting more loss in mass and carbonate during dissolution with modifications of A-, B-, and labile CO<sub>3</sub><sup>2-</sup> amounts during recrystallization which were dependent on the initial apatite CO<sub>3</sub><sup>2</sup>- content. Meanwhile, apatites exposed to KCl had less mass loss during dissolution and retained the crystal structure, A-, B-, and labile CO<sub>3</sub><sup>2-</sup> amounts during recrystallization, suggesting that K<sup>+</sup> may shield apatites from dissolution. To our knowledge, this is the first study to parse out mechanistic differences between Na<sup>+</sup> and K<sup>+</sup> on biomimetic carbonated apatite dissolution/recrystallization. Overall, this study will provide insight on how fluctuating Na<sup>+</sup> and K<sup>+</sup> in saliva may affect tooth mineral composition and structure.

Keywords: B Spectroscopy, C Chemical properties, D Apatite, E Biomedical Applications, B Impurities

## 1. Introduction

Teeth are continuously bathed in saliva. Saliva is a complex fluid with an ever-changing composition. These changes depend on many factors, including time of day, stress [1], diet [2,3], and health conditions such as hyposalivation [4], aging [5], diabetes [6], and chronic kidney disease [7]. Two of the primary ionic components in saliva are sodium (Na<sup>+</sup>) and potassium (K<sup>+</sup>). These can fluctuate in concentration between 11.5-271.9 mM and 2.6-27.4 mM, respectively[1–7]. The changes in salivary ionic composition give way to modified ionic exchange mechanisms between the surrounding saliva and tooth mineral [8].

Enamel and dentin are primarily composed of calcium-deficient carbonate-substituted apatite mineral [8–10]. This mineral is known for allowing substitutional ionic exchanges within its structure [11]. Some of these include cationic substitutions of Na<sup>+</sup> and K<sup>+</sup>. Na<sup>+</sup> can easily substitute for calcium (Ca<sup>2+</sup>) due to its similar ionic sizes (1.02 for Na<sup>+</sup> vs 1.00 for Ca<sup>2+</sup> for ionic radii size [12,13]. On the other hand, K<sup>+</sup> has more difficulty substituting into the mineral lattice for Ca<sup>2+</sup> due to its larger ionic radius (1.38) [13]. Since these monovalent ions substitute for the divalent Ca<sup>2+</sup> ion, Na<sup>+</sup> and K<sup>+</sup> must be co-substituted with another ion, typically carbonate (CO<sub>3</sub><sup>2-</sup> ), to maintain charge balance [13]. For Na and CO<sub>3</sub><sup>2</sup>- coupled substitutions, previous studies have extensively identified the molecular interactions between Na<sup>+</sup> and CO<sub>3</sub><sup>2-</sup> with most studies concluding the importance of Na<sup>+</sup> within the apatite structure [14–17]. Other studies have also identified K<sup>+</sup> sole effect on the apatites structure [18,19], albeit to a lesser extent, with little information about its coupled substitution with CO<sub>3</sub><sup>2-</sup> compared to Na<sup>+</sup> [20,21]. Recently, our lab discovered that co-substitutions of Na<sup>+</sup> or K<sup>+</sup> with CO<sub>3</sub><sup>2-</sup> modifies the location of the CO<sub>3</sub><sup>2-</sup> within the apatite lattice, such as increased A-type CO<sub>3</sub><sup>2-</sup> in apatites synthesized with K<sup>+</sup> compared to Na<sup>+</sup> [22]. This resulted in modifications to the mineral structure and physiochemical properties.

CO<sub>3</sub><sup>2-</sup> substitution is one of the most common anionic substitutions in enamel and dentin. Enamel contains about 2 wt% CO<sub>3</sub><sup>2-</sup>, while dentin has ~5-7 wt% CO<sub>3</sub><sup>2-</sup> [8,9,23]. These carbonate ions can substitute in multiple places within the apatite structure. Carbonate can exchange for phosphate, known as B-type CO<sub>3</sub><sup>2-</sup>, and/or for the hydroxyl groups, known as A-type CO<sub>3</sub><sup>2-</sup>, within the crystalline core [24–26]. Carbonate can also reside in the amorphous hydrated layer, known as labile CO<sub>3</sub><sup>2-</sup> [24,27]. Changes in CO<sub>3</sub><sup>2-</sup> content and location can modify the morphological, structural, and chemical characteristics of apatite [25,28–30]. For example, increased B-type CO<sub>3</sub><sup>2-</sup> substitutions increase the mineral solubility and decrease the crystallinity [29,31], crystallite size [31,32] and stiffness [33]. Additionally, these substitutions change the atomic lattice spacing along both the a- and c-axes [28,29]. As it has previously been shown that Na<sup>+</sup> and K<sup>+</sup> can modify CO<sub>3</sub><sup>2-</sup> co-substitutions within the apatite lattice, this suggests that substitutions of Na<sup>+</sup> and K<sup>+</sup> that affect CO<sub>3</sub><sup>2-</sup> locations and concentrations could have significant effects on the solubility, structure, and mechanics of tooth minerals.

In addition to its effect on CO<sub>3</sub><sup>2-</sup>, Na<sup>+</sup> and K<sup>+</sup> have also been shown to affect the crystallization and growth of calcium phosphates. For example, previous studies have shown that NaCl and KCl solutions have distinct differences on calcium phosphate crystal growth [34], nucleation rate [35], and crystal shape [35]. In addition, Na<sup>+</sup> incorporation during crystallization

affects physiochemical properties of apatite, such as  $CO_3^{2-}$  vibrations [15,36]. Despite knowing that  $Na^+$  and  $K^+$  can affect mineral growth, structure, and composition - much like other ionic components such as  $Mg^+$  and  $F^-$  [37–39] - it is unknown how they affect biomimetic carbonated apatites after formation. Therefore, the goal of this study was to determine how extant biomimetic carbonated apatite is altered during exposure to  $Na^+$  and  $K^+$ -rich solutions that simulate the concentrations range of  $Na^+$  and  $K^+$  within saliva. This study will provide insight as to how tooth mineral may react during salivary variations in  $Na^+$  or  $K^+$  content.

## 2. Methods

### 2.1. Synthesis

To mimic the carbonate content in enamel and dentin, biomimetic apatite powders were synthesized through an aqueous precipitation reaction with an aim to obtain ~3 and ~7 wt% carbonate as previously described [29]. In short, 50 mL of 0.15 M calcium nitrate tetrahydrate (ACROS, USA), 50 mL of 0.09 M sodium phosphate (ACROS, India) were slowly titrated drop by drop into a 250 mL of either 0 mM or 6 mM sodium bicarbonate (Sigma-Aldrich, France) for 3 or 7 wt% CO<sub>3</sub><sup>2-</sup> substitution, respectively, at 60°C. The low and high wt% of CO<sub>3</sub><sup>2-</sup> represents enamel and dentin, respectively. The pH was maintained at ~pH 9 with 0.1 M NaOH (ACROS, Sweden). Once completely titrated, the mixture was left to mature for 2 hours at ~pH 9 at 60°C. Afterwards, the precipitate was filtered, rinsed thoroughly, and dried at 60°C overnight. X-Ray Diffraction and Raman Spectroscopy was used to confirm the apatitic phase with carbonate substitutions. The amount of carbonate was determined by comparing the carbonate to phosphate ratio to our standardized carbonate apatites that were correlated to the carbon amount determined by Carbon Hydrogen Nitrogen [29].

## 2.2. Dissolution/exposure experiment

50 mg of apatite with either 3% or 7% substituted carbonate was placed into 10 mL of either sodium chloride or potassium chloride in conical tubes. 3 concentrations of sodium chloride (Fisher, USA) or potassium chloride (Sigma-Aldrich, USA) were used: 0.05 M, 0.1 M, 0.2 M, at 2 different pH's, pH 5.5 and pH 7.4 (Supplemental Figure 1) to represent low and high amounts of Na<sup>+</sup> or K<sup>+</sup> concentrations at acidic and neutral pH's that can occur in the mouth [40,41]. The powders were exposed to the solutions for 3 days and the pH of the solutions were obtained at 1, 3, 6, 24, 48, and 72 hours. After 3 days, the powders were filtered with P4 filter paper (Fisher Scientific, China), rinsed with 10 mL of Millipore water 3 times, and dried at 60°C overnight. The powders were massed to determine the mass lost during the exposure period. Each condition had 3 replicates.

## 2.3. Raman Spectroscopy

The composition of the powders was initially determined by using Raman spectroscopy. Using a WiTec alpha300 with a 785 nm laser, 10 points per sample were obtained at an acquisition time of 1 second for 30 accumulations. The following peaks were fit using the Lorentzian fit function of WiTec Program 5.1 to obtain the following peak areas:  $v_3 PO_4^{3-}$  (430 cm<sup>-1</sup>),  $v_4 PO_4^{3-}$  (590 cm<sup>-1</sup>),  $v_1 PO_4^{3-}$  (950 cm<sup>-1</sup>),  $v_1 PO_4^{3-}$  (960 cm<sup>-1</sup>),  $v_2 PO_4^{3-}$  (1050 cm<sup>-1</sup>), and  $v_1 CO_3^{2-}$  (1070 cm<sup>-1</sup>). The carbonate to phosphate ratio ( $CO_3/PO_4$ ) was calculated from the ratio of

the 1070/(950+960) peak areas for each sample to determine the percent change in  $CO_3/PO_4$  (% $\Delta$   $CO_3/PO_4$ ) [29,42,43]. Each condition had 3 replicates.

## 2.4. Fourier Transform Infrared Spectroscopy

Attenuated Total Reflectance (ATR) FTIR spectroscopy was used to confirm the apatite characteristic phase and determine the amount of A-type, B-type, and labile CO<sub>3</sub><sup>2-</sup> in the apatites before and after exposure. Using a Nicolet Magna-IR 500 spectrometer, each powder had an acquisition of 64 scans with a resolution of 2 cm<sup>-1</sup> from 400-4000 cm<sup>-1</sup>. Using the OriginPro 2021b software (OriginLab Corporation, Northampton, MA, USA), the v<sub>2</sub> CO<sub>3</sub><sup>2-</sup> peak within the 900-750 cm<sup>-1</sup> range were deconvoluted for the A-type, B-type, and labile CO<sub>3</sub><sup>2-</sup> peaks with the respective initial peak centers of 880 cm<sup>-1</sup>, 873 cm<sup>-1</sup>, 867 cm<sup>-1</sup> using a Gaussian fit function [15]. Each condition had 3 replicates.

## 2.5. X-Ray Diffraction

The structure and phase of the powders were determined by X-ray Diffraction. Each sample was analyzed from 20-60° 20 with 0.02° step with 1 second per step using a Bruker D2 Phaser Diffractometer (Bruker AXS, Germany) operating at 30 kV and 10 mA. 11 peaks were deconvoluted using a PseudoVoigt function with the Diffrac.Eva software to determine the peak centers, full width at half max (FWHM), crystallite length and width, and lattice spacing of the apatites before and after solution exposure. The d-spacing for the 002, 310, and 004 planes were scrutinized. Afterwards, the crystallite length and width determined by the 002 and 310 planes respectively were determined via Scherrer's equation using the peak FWHM. The powders were compared against stoichiometric hydroxyapatite from the Powder Diffraction File from the International Centre for Diffraction Data (ICDD). Each condition had 3 replicates.

## 2.6. Inductively Coupled Plasma – Optical Emission Spectroscopy (ICPOES)

One solution sample from each condition (n=1) was analyzed for changes in calcium (Ca), phosphorus (P), sodium (Na), and potassium (K) before and after solution exposure via a Perkin Elmer 7300DV Dual View Inductively Coupled Plasma–Optical Emission Spectrometer (ICP-OES). All samples were directly analyzed at 20x dilution due to the very high levels of phosphate in the samples. Standard quality assurance procedures were employed, including analysis of initial and continuing calibration checks and blanks, duplicate samples, preparation blanks (Blank), post digestion spiked samples, and laboratory control samples (LCS).

## 2.7. Statistical Analyses

Multiway Analysis of Variance (ANOVA) with Tukey test comparison was used in OriginPro 2021b (OriginLab Corporation, Northampton, MA, USA) to determine the statistical significance for the aforementioned quantitative analyses and between the independent variables of pH, concentration,  $Na^+$  vs  $K^+$ , and wt%  $CO_3^{2-}$ . Significance is classified as p<0.05.

## 3. Results

#### 3.1. pH

The change in solution pH ( $\Delta$ pH) with mineral exposure was significantly higher when the solution had an initial pH of 5.5 (pH<sub>i</sub> 5.5) compared to pH<sub>i</sub> 7.4 (Figure 1A and Supplemental

Table 1). The average  $\Delta pH$  was between 1.48 and 2.49 for the 3%  $CO_3^{2-}$  apatites at  $pH_i$  5.5 and between 1.81 and 3.02 for 7%  $CO_3^{2-}$  apatites at  $pH_i$  5.5. This is 15X larger than the average  $\Delta pH$  for  $pH_i$  7.4 which ranged from -0.12 to 0.20 for 3%  $CO_3^{2-}$  and -0.13 to 0.92 for 7%  $CO_3^{2-}$ .

Regarding the solution cationic concentration, the increase in [Na<sup>+</sup>] or [K<sup>+</sup>] molar concentrations generally decreased the  $\Delta pH$  overall at all pH's and wt%  $CO_3^{2^-}$ . However, the differences were only statistically significant for 0.05 M concentrations for both Na<sup>+</sup> and K<sup>+</sup> when considering pH and wt%  $CO_3^{2^-}$  as factors (Supplemental Table 2).  $\Delta pH$  of the solution when mineral was added to water was the lowest value in nearly all cases, contrary to the trend suggesting that increased cationic content reduced  $\Delta pH$ .

When comparing crystals containing either 3% or 7% substituted  $CO_3^{2-}$  at all conditions, the 7%  $CO_3^{2-}$  samples induced a significantly larger  $\Delta pH$  in all solutions compared to their 3%  $CO_3^{2-}$  counterparts (Supplemental Table 3). Similarly, when comparing the effect of KCl versus NaCl, the KCl solutions exhibited a significantly larger  $\Delta pH$  than their NaCl and water counterparts when factoring wt%  $CO_3^{2-}$  and pH (Supplemental Table 4). Conversely, there was no significant difference between NaCl and water.

#### 3.2. Mass

KCl had significantly less mineral mass lost after exposure than NaCl at both 3% and 7%  $\rm CO_3^{2-}$  (Figure 1B and Supplemental Tables 5-6). For 3%  $\rm CO_3^{2-}$ , there's roughly 20% more mass loss in NaCl than KCl, while NaCl had 40-50% more mass loss than KCl at 7%  $\rm CO_3^{2-}$ . There were no apparent trends with concentration or pH in mass lost. However, more mass was lost at 3%  $\rm CO_3^{2-}$  than 7% for KCl as well as NaCl (Supplemental Tables 7-8).

#### 3.3. Raman – Carbonate content

Overall, the % $\Delta$ CO3/PO4 was significantly higher for the mineral placed in KCl than in NaCl at 3 wt% CO<sub>3</sub><sup>2-</sup>, indicating higher amounts of CO<sub>3</sub><sup>2-</sup> in the mineral in KCl (Figure 2 and Supplemental Table 9). For NaCl solution exposures, the % $\Delta$ CO3/PO4 was generally unchanged at pH 5.5 for apatites with an initial 3% and 7% CO<sub>3</sub><sup>2-</sup> substitution. However, the % $\Delta$ CO3/PO4 was significantly elevated for crystals containing 3% CO<sub>3</sub><sup>2-</sup> compared to 7% CO<sub>3</sub><sup>2-</sup> at pH 7.4 (Supplemental Table 10). For the mineral exposed to KCl, the % $\Delta$ CO3/PO4 significantly increased about ~20-30% at both pHs and at all concentrations for 3 wt% CO<sub>3</sub><sup>2-</sup> compared to 7% CO<sub>3</sub><sup>2-</sup> (Supplemental Table 11).

## 3.4. FTIR - Carbonate type

Raman established that the apatite crystals placed in KCl had higher  $CO_3^{2-}$  content than apatite placed in NaCl especially for crystals with low starting  $CO_3^{2-}$  (3%). FTIR data indicates that this may be due to shifts in the  $CO_3^{2-}$  environment within the crystal lattice. For 3 wt%  $CO_3^{2-}$  for apatites exposed to all solutions, the relative amounts of A-type  $CO_3^{2-}$  generally did not change after being exposed to all pH's and concentrations (Figure 3A). At an initial 7 wt%  $CO_3^{2-}$  content, the amount of A-type  $CO_3^{2-}$  generally decreased for apatites exposed to NaCl at all concentrations and pHs compared to the unexposed powder (Ctrl); however, no apparent trends in terms of concentrations nor pH were observed. For apatites with an initial 7 wt%  $CO_3^{2-}$ , there

were no changes in  $CO_3^{2-}$  content as a function of  $CO_3^{2-}$  location. In addition, there were no changes in A-type  $CO_3^{2-}$  between the 3% and 7%  $CO_3^{2-}$  unexposed control groups.

The 7 wt%  $CO_3^{2-}$  unexposed control had higher levels of B-type  $CO_3^{2-}$  compared to the 3 wt% control as expected (Figure 3B). For 3 wt%  $CO_3^{2-}$ , apatites placed in water generally increased in B-type  $CO_3^{2-}$  at both pH's. At the same  $CO_3^{2-}$  content, apatites exposed to NaCl showed a decreasing trend in B-type  $CO_3^{2-}$  compared to controls at both pH's, while apatites in KCl retained the same amount of B-type  $CO_3^{2-}$  at all concentrations and pH's except 0.05 M KCl at pH 5.5. Three wt%  $CO_3^{2-}$  apatites placed in NaCl exhibited less B-type  $CO_3^{2-}$  than those in KCl. For apatites with an initial 7 wt%  $CO_3^{2-}$ , there were no changes or trends in B-type content after exposure for all solutions, concentrations, and pHs.

For the unexposed samples (Ctrl), the relative amounts of labile  ${\rm CO_3}^{2-}$  decreased as the initial wt%  ${\rm CO_3}^{2-}$  increased (Figure 3C). At 3 wt%  ${\rm CO_3}^{2-}$ , apatites exposed to NaCl showed a trending increase in labile  ${\rm CO_3}^{2-}$  compared to the unexposed control sample while KCl samples generally showed no changes and water samples showed a trending decrease in labile  ${\rm CO_3}^{2-}$ . Contrarily, there were no changes in labile  ${\rm CO_3}^{2-}$  at 7 wt%  ${\rm CO_3}^{2-}$  after exposure to all conditions.

#### 3.5. XRD – Structure

The apatites before exposure to the solutions exhibited an average d-spacing of 3.445 and 3.444 along the 002 (c-axis) for 3 and 7 wt% CO<sub>3</sub><sup>2-</sup>, respectively, while the average 310 (a-axis) d-spacing was 2.273 and 2.264 (Figure 4A-B). The increased c-axis spacing and the decreased a-axis between the initial 3% and 7% CO<sub>3</sub><sup>2-</sup> apatites agrees with previously reported trends for B-type apatites [29]. For 3 wt% CO<sub>3</sub><sup>2-</sup> apatites exposed to NaCl, the c-axis and a-axis showed a trending decrease compared to the unexposed control apatite at pH 7.4. However, there were no statistically significant differences in the mineral c-axis or a-axis spacing as a function of any of the independent variables.

For crystallite size, 3% CO<sub>3</sub><sup>2-</sup> had a significantly higher crystallite length and width along the c-axis and a-axis, respectively, compared to 7% CO<sub>3</sub><sup>2-</sup> for all variables as expected (Figure 5A-B and Supplemental Tables 12-13) [29,44]. 3% CO<sub>3</sub><sup>2-</sup> apatite at all conditions had between 230.04-321.72 nm in crystallite length with no significant changes between conditions. 7% CO<sub>3</sub><sup>2-</sup> apatite in all conditions had between 106.30-189.09 nm in crystallite length (Figure 5A) with no significance between changes as well. Additionally, NaCl exhibited a trend of higher crystallite length than KCl, specifically at pH 7.4 at all wt% CO<sub>3</sub><sup>2-</sup> as well as 7% CO<sub>3</sub><sup>2-</sup> at pH 5.5. There were no trends with concentration or pH at either wt% CO<sub>3</sub><sup>2-</sup> or within NaCl and KCl.

The crystallite width for 3 wt%  $CO_3^{2-}$  apatites exposed to water increased in water at pH 5.5 and 7.4 (Figure 5B). The crystallite width also increased for 3 wt%  $CO_3^{2-}$  in NaCl at pH 7.4 as compared to unexposed control while the width either stayed the same or decreased in KCl. For apatites with an initial 7 wt%  $CO_3^{2-}$ , no changes were observed for apatites exposed to water and KCl. Contrarily, the width significantly increased for all NaCl conditions compared to KCl (Supplemental Table 14).

#### 3.6. ICP-OES – Ionic content of solutions

The solutions before and after exposure to the apatite powders were analyzed for  $Ca^{2+}$ , P,  $Na^+$ , and  $K^+$  content through ICP-OES to determine the change of solutes ( $\Delta Ca$ ,  $\Delta P$ ,  $\Delta Na$ , and  $\Delta K$ ).  $\Delta Ca$  and  $\Delta P$  increased in the solution at all conditions for 3 and 7 wt%  $CO_3^{2-}$ , indicating an increase of  $Ca^{2+}$  and P after exposure to the apatite powders (Figure 6A-B). While 3%  $CO_3^{2-}$  apatites were generally similar in  $Ca^{2+}$  and P content in the solution after exposure to the powders, 7 wt%  $CO_3^{2-}$  apatites in NaCl at pH 5.5 as well as water at both pH's had an increased  $Ca^{2+}$  and P content in the solution compared to NaCl pH 7.4 and KCl at all conditions. There were generally no significant changes between KCl at all conditions at 7 wt%  $CO_3^{2-}$ .

As expected,  $\Delta$ Na content did not change in the solution for water and KCl for 3 and 7 wt%  $CO_3^{2^-}$  apatites, irrespective of pH and concentration (Figure 6C). Na<sup>+</sup> content in the solution with 7 wt%  $CO_3^{2^-}$  generally did not change as well. However, for NaCl solutions with 3%  $CO_3^{2^-}$  apatites, the amount of Na<sup>+</sup> in the solution decreased, especially for pH 7.4 with increasing NaCl concentration.

Conversely, K<sup>+</sup> content in the solution did not change for NaCl irrespective of wt% CO<sub>3</sub><sup>2</sup>, concentration, and pH after exposure to the powders as expected (Figure 6D). There were inconsistent changes with KCl, exhibiting a range of either relatively low to high increases or decreases of K<sup>+</sup> content in the solution for both wt% CO<sub>3</sub><sup>2-</sup>.

#### 4. Discussion

Teeth are mainly composed of dynamic carbonated apatite mineral which is subjected to many ionic fluctuations in the surrounding salivary fluid, such as variations in Na<sup>+</sup> or K<sup>+</sup> concentration. Because the apatite mineral easily allows substitutions to occur, these Na<sup>+</sup> and K<sup>+</sup> ions can integrate, ultimately changing the composition and mineral structure [20,22]. While many previous studies by others and ourselves have determined that Na<sup>+</sup> increases B-type CO<sub>3</sub><sup>2</sup>incorporation into apatites during formation [22,45,46], we recently discovered that K<sup>+</sup> can increase the amount of A-type CO<sub>3</sub><sup>2</sup>- substitution during bone-like apatite synthesis [22]. These different co-substitutions within apatite ultimately changed the lattice structure and carbonate environment despite the lower K<sup>+</sup> incorporation into apatite compared to Na<sup>+</sup>. Previous studies have also shown that NaCl and KCl solutions can affect crystal growth of calcium phosphates differently, in which increased NaCl concentration increased the crystal growth rate compared to KCl [35]. However, the growth rate decreases when seeded crystals were placed in NaCl [34]. While these studies have looked at the effects of Na<sup>+</sup> and K<sup>+</sup> during synthesis, crystallization, and growth, it is important to understand how Na<sup>+</sup> and K<sup>+</sup> in the solution affect pre-existing carbonated apatites after crystallization. In this study, to better understand this behavior, biomimetic apatites with 3 and 7 wt% CO<sub>3</sub><sup>2</sup> were exposed to increasing NaCl or KCl concentrations with either pH 5.5 or 7.4 to represent possible variations in salivary chemistry.

When the apatite crystals were exposed to NaCl solutions, the significant increase in pH, especially at initially low starting pH (pH<sub>i</sub>), was expected as acidic solutions increase apatite dissolution and release larger concentrations of buffering ions, such as  $CO_3^{2-}$  and  $PO_4^{3-}$  (Figure 1) [44,47–49]. Apatite dissolution in NaCl was confirmed by the reduction of crystal mass and

increase of  $Ca^{2+}$  and P in the solution after exposure for both pHs and initial wt%  $CO_3^{2-}$  (Figure 6A-B). Along with a loss of mass (Figure 1B), apatite exposed to lower pHs has been associated with decreased mineral  $CO_3^{2-}$  content [44,49]. Indeed, at low pH<sub>i</sub>, both the 3 and 7%  $CO_3^{2-}$  apatites exhibit a decrease in  $CO_3^{2-}$  with exposure, indicating that  $CO_3^{2-}$  was released from apatite to increase the solution pH (Figure 2). At pH 7.4, the increased or lack of change within the mineral  $CO_3^{2-}$  content correlates with the lack of change in  $\Delta$ pH at the elevated pH<sub>i</sub> (Figure 1A). This suggests that less dissolution was occurring for apatites in NaCl at higher pHs, agreeing with previous studies [44]. Together, these results point to a classical dissolution phenomena in NaCl in which the apatite mineral dissolves by releasing buffering ions, specifically  $CO_3^{2-}$ , to increase the solution pH.

CO<sub>3</sub><sup>2-</sup> can substitute into three separate locations in the apatite mineral crystal and it is unclear which locations are preferentially affected by solution exposure. For apatites in NaCl, the initial crystal composition played an essential role in determining which CO<sub>3</sub><sup>2</sup> was most affected by solution exposure. The general loss of B-type  $CO_3^{2-}$  for 3 wt%  $CO_3^{2-}$  apatites in NaCl for all concentrations indicates that the mineral crystals were undergoing dissolution with a preferential removal of B-type CO<sub>3</sub><sup>2-</sup> when initially exposed to the NaCl solutions (Figure 3B-C). This was supported by the decrease in the c-axis spacing, particularly seen in the 3% CO<sub>3</sub><sup>2-</sup> apatite exposed to NaCl at pH 7.4 as compared to the unexposed crystals (Figure 4A) [29]. The increased labile CO<sub>3</sub><sup>2</sup>- suggests that the CO<sub>3</sub><sup>2</sup>- in solution may be integrated through ionic exchange in the hydrated layer once recrystallization occurs [27]. In addition, the general decrease of Na<sup>+</sup> content in the solution (Figure 6C) suggests that the initial 3 wt% CO<sub>3</sub><sup>2-</sup> is likely taking up Na<sup>+</sup> from the solution in conjunction with the change in CO<sub>3</sub><sup>2-</sup> content during recrystallization. Conversely, the 7% CO<sub>3</sub><sup>2-</sup> apatite exhibited fewer modifications of the CO<sub>3</sub><sup>2-</sup> content with exposure than the 3% CO<sub>3</sub><sup>2</sup>- apatite (Figure 2). In these apatites, the lack of change in labile and B-type with only general decreases in A-type CO<sub>3</sub><sup>2-</sup> content suggests that the higher carbonated mineral preferentially releases the CO<sub>3</sub><sup>2-</sup> in the apatite channels when exposed to NaCl (Figure 3B-C) [36]. This agrees with previous studies indicating a relationship between A-type CO<sub>3</sub><sup>2-</sup> and Na<sup>+</sup> for highly carbonated apatites synthesized at higher temperatures as created in this study [15]. Due to the small amount of A-type dissolved, the lattice spacing was not affected (Figure 3A). Regardless of the location of the carbonate loss, the increased crystallite size for crystals exposed to NaCl compared to the unexposed crystals (Figure 5A-B) may be explained by the CO<sub>3</sub><sup>2</sup>removal from the lattice as this may lead to the formation of less distorted crystals, which reduces the crystal energy and promotes crystal growth [29,50,51]. Overall, exposure of apatite to NaCl solutions resulted in larger apatite crystals with modified CO<sub>3</sub><sup>2-</sup> distributions that are dependent on the initial apatite composition itself, rather than pH or NaCl concentration.

Apatite crystals in NaCl exhibited the expected behaviors of a conventional dissolution/recrystallization and release of buffering ions; however, this was not the case for KCl. Much like in NaCl, the presence of mineral in KCl increased the solution pH, indicating that buffering ions may be released (Figure 1A). The  $\Delta pH$  also increased with reduced pH<sub>i</sub> and reduced KCl concentration as seen with NaCl. However, the similarities end there. The significantly less mass lost in apatite in KCl compared to its NaCl counterpart (Figure 1B) suggests that the increase in solution pH is not caused by mineral dissolution. Instead, K<sup>+</sup> may

have protective effects against dissolution of apatite itself [52,53]. Furthermore, the  $3\% \text{ CO}_3^{2-}$ apatite did not exhibit the expected loss of CO<sub>3</sub><sup>2</sup> with exposure like NaCl (Figure 1B and Figure 2). Instead, the CO<sub>3</sub><sup>2-</sup> levels in apatite increased with KCl exposure, further supporting the expected decrease in crystallite size with increasing CO<sub>3</sub><sup>2-</sup> (Figure 5A-B). Without apatite dissolution or the release of CO<sub>3</sub><sup>2-</sup> buffering ions, the measured increase in pH may be caused by the sequestration of protons (H<sup>+</sup>) in the metastable hydrated surface layer and/or the protonated states of PO<sub>4</sub><sup>3-</sup> or CO<sub>3</sub><sup>2-</sup> to create HPO<sub>4</sub><sup>2-</sup> and HCO<sub>3</sub><sup>-</sup> substitution in the apatite lattice or within the hydrated layer [36,54–56]. To elaborate, the final pH for all conditions was ~pH 7, resulting in the ionization of the solution PO<sub>4</sub><sup>3-</sup> into HPO<sub>4</sub><sup>2-</sup>. HPO<sub>4</sub><sup>2-</sup> is known to integrate within the Btype sites to replace  $CO_3^{2-}$  in the lattice as well as within the amorphous apatite surface layer [27,55,57]. This may provide a possible explanation for the dissolution-free buffering. Accumulation of positively charged H<sup>+</sup> into the hydrated layer could also recruit negatively charged CO<sub>3</sub><sup>2</sup>, which may explain both the buffering and the increased CO<sub>3</sub><sup>2</sup> content. Overall, this data suggests that having K<sup>+</sup> in the solution may be protective against dissolution of apatites compared to the dissolving nature of Na<sup>+</sup> solutions as seen in this study. To our knowledge, this is the first time that this behavior has been described.

With so many possible ion exchanges, it was necessary to determine how KCl exposure affected the location of the CO<sub>3</sub><sup>2</sup>. Once again, exposure to KCl had significantly different effects on CO<sub>3</sub><sup>2</sup>- location than NaCl. The 3% CO<sub>3</sub><sup>2</sup>- apatites in KCl showed a general decrease in A-type CO<sub>3</sub><sup>2</sup>- and an increase in B-type CO<sub>3</sub><sup>2</sup>- compared to the unexposed mineral (Figure 3A). It previously has been shown that the presence of K<sup>+</sup> during crystal formation shifts the location of CO<sub>3</sub><sup>2</sup> away from the B-type location and into the A-type locations [22], the opposite of what was seen here. This data indicates that the K<sup>+</sup> in the KCl is likely not integrating into the lattice of the exposed apatites, but it may be serving as a protective barrier in the solution instead, perhaps in a Stern-like layer [58,59] or in the hydrated layer. The K<sup>+</sup> levels in the solution showed mixed results supporting the idea that there is no significant exchange of K<sup>+</sup> between the solution and the mineral lattice (Figure 6D). Interestingly, the increase in B-type CO<sub>3</sub><sup>2-</sup> did not significantly affect the lattice spacing of the crystals (Figure 4A). This could be due to the smaller number of CO<sub>3</sub><sup>2</sup> exchanges in the KCl sample as compared to the NaCl samples. In addition, the lack of change of labile CO<sub>3</sub><sup>2-</sup> in the hydrated layer for the 3% CO<sub>3</sub><sup>2-</sup> apatites in KCl (Figure 3C) may point to an increased uptake of H<sup>+</sup> in the hydrated layer. Because HPO<sub>4</sub><sup>2-</sup> substitutes for the PO<sub>4</sub><sup>3-</sup> groups/B-type sites within apatite, this may be through protonation of HCO<sub>3</sub><sup>-</sup> or HPO<sub>4</sub><sup>2</sup><sup>-</sup> – as a better mechanism for reducing H<sup>+</sup> in the solution than HPO<sub>4</sub><sup>2-</sup> substitution within the lattice. At an initial 7% CO<sub>3</sub><sup>2</sup>, the apatites exhibited no change in A, B, or labile-type apatite with exposure, further supporting the idea that K<sup>+</sup> acts as a protectant to the mineral crystals, compared to Na.

In terms of the independent variables of pH and concentration, there were surprisingly few correlations with mineral properties. The concentration of both NaCl and KCl as well as the pH $_i$  significantly affected the  $\Delta pH$  of the solution (Figure 1A). In addition, the pH $_i$  may have had slight effects on the CO $_3$ <sup>2-</sup> content and location. However, these were rarely the primary factors responsible for the measured changes in mineral properties. It is possible that the time frame of 3 days and the rapid increase from pH 5.5 to  $\sim$ pH 7-8, especially for KCl, may explain the lack of effect of pH $_i$  as the mineral in all conditions generally equilibrated within the first hour

(Supplemental Figure 2-3). Previously, the initial pH exhibited more significant effects in solutions with high buffering capacities unlike the ones used here [60]. Instead, these apatites behaved more like apatite dissolution in water [44]. In terms of concentration, it has previously been shown that the effect of concentration on the dissolution properties of apatite is dependent on the type of simple salt [61], where NaCl may have relatively little effect on the dissolution mechanism supporting the data collected here.

#### 4.1. Limitations

Biological and biomimetic carbonated apatites have a substantial amount of HPO<sub>4</sub><sup>2-</sup> in the hydrated surface layer and within the crystalline apatite core [24]. Due to the increased pH, low mass loss, and increased CO<sub>3</sub><sup>2-</sup> content after exposure, HPO<sub>4</sub><sup>2-</sup> may contribute to ionic substitution and dissolution in this study. Therefore, future studies determining the role of HPO<sub>4</sub><sup>2-</sup> in Na<sup>+</sup>- and K<sup>+</sup>-rich solutions will be important to understand the mechanism.

In addition, the solutions used here did not include other ions such as phosphate. Phosphate is a necessary component of saliva as well as other solutions used in medical research laboratories to prevent dissolution and alteration of mineral and calcified tissues [49,62,63]. Thus, future studies identifying this mechanism will be needed to fully understand carbonated apatite mineral dissolution in Na- and K-rich solutions with physiological phosphate conditions.

Furthermore, the conditions shown here were performed in triplicate. While the standard deviations were relatively small for most of the dependent factors, more replicates would be needed in future studies to further determine the statistical power.

#### 5. Conclusions

The effect of variations in solution pH and cationic content on biomimetic tooth mineral structure and composition was investigated. It was found that, Na<sup>+</sup> causes dissolution of the mineral, resulting in greater release of CO<sub>3</sub><sup>2-</sup> (primarily B-type CO<sub>3</sub><sup>2-</sup> at low initial wt% CO<sub>3</sub><sup>2-</sup> and primarily A-type CO<sub>3</sub><sup>2-</sup> at high starting CO<sub>3</sub><sup>2-</sup> wt%), which increases the crystallite length and width as well as decreases the overall mass. This suggests that the apatite mineral undergoes classical dissolution and recrystallization in Na-rich solutions. On the other hand, KCl appears to protect the mineral from dissolution, resulting in less mass loss after exposure and retention of A-type, B-type, and labile CO<sub>3</sub><sup>2-</sup> as well as the crystalline lattice. Despite this lack of dissolution, the apatite was still able to buffer the acidic solutions likely because of H<sup>+</sup> sequestration. Revealing the phenomena between Na<sup>+</sup>, K<sup>+</sup>, and biomimetic apatites could aid in the development of treatments for the prevention of tooth dissolution. It also may provide some insight as to why K-rich diets aid in bone health while Na-rich diets are detrimental to bone.

## 6. Acknowledgements

We would like to acknowledge the Center for Environmental Science and Engineering (CESE) and the Institute of Materials Science (IMS) at the University of Connecticut for their assistance. Funding was provided by the University of Connecticut's Summer Dental Research Program for Katherine Peccerillo as well as the NSF CAREER grant [grant number 2044870] for Alix Deymier.

#### 7. References

- [1] G. Singh, E. Iyer, H. Malik, Relative Changes in Salivary Sodium and Potassium in Relation to Exposure to High G Stress, Med J Armed Forces India 50 (1994) 261–265. https://doi.org/10.1016/S0377-1237(17)31082-1.
- [2] N.A. Thorn, I.L. Schwartz, J.H. Thaysen, Effect of Sodium Restriction on Secretion of Sodium and Potassium in Human Parotid Saliva, Journal of Applied Physiology 9 (1956) 477–480. https://doi.org/10.1152/jappl.1956.9.3.477.
- [3] C. Simões, I. Caeiro, L. Carreira, F.C. e Silva, E. Lamy, How Different Snacks Produce a Distinct Effect in Salivary Protein Composition, Molecules 26 (2021) 2403. https://doi.org/10.3390/molecules26092403.
- [4] A. Almståhl, M. Wikström, Electrolytes in stimulated whole saliva in individuals with hyposalivation of different origins, Archives of Oral Biology 48 (2003) 337–344. https://doi.org/10.1016/S0003-9969(02)00200-5.
- [5] C. Labat, S. Thul, J. Pirault, M. Temmar, S.N. Thornton, A. Benetos, M. Bäck, Differential associations for salivary sodium, potassium, calcium, and phosphate levels with carotid intima media thickness, heart rate, and arterial stiffness, Disease Markers 2018 (2018). https://doi.org/10.1155/2018/3152146.
- [6] B. Kallapur, K. Ramalingam, Bastian, A. Mujib, A. Sarkar, S. Sethuraman, Quantitative estimation of sodium, potassium and total protein in saliva of diabetic smokers and nonsmokers: A novel study, J Nat Sci Biol Med 4 (2013) 341–345. https://doi.org/10.4103/0976-9668.117006.
- [7] T. Dhondup, Q. Qian, Acid-Base and Electrolyte Disorders in Patients with and without Chronic Kidney Disease: An Update, Kidney Diseases 3 (2017) 136–148. https://doi.org/10.1159/000479968.
- [8] E.A.A. Neel, A. Aljabo, A. Strange, S. Ibrahim, M. Coathup, A.M. Young, L. Bozec, V. Mudera, Demineralization–remineralization dynamics in teeth and bone, International Journal of Nanomedicine 11 (2016) 4743–4763. https://doi.org/10.2147/IJN.S107624.
- [9] A.B. Sønju Clasen, I.E. Ruyter, Quantitative determination of type A and type B carbonate in human deciduous and permanent enamel by means of Fourier transform infrared spectrometry., Advances in Dental Research 11 (1997) 523–527. https://doi.org/10.1177/08959374970110042101.
- [10] J. De Dios Teruel, A. Alcolea, A. Hernández, A.J.O. Ruiz, Comparison of chemical composition of enamel and dentine in human, bovine, porcine and ovine teeth, Archives of Oral Biology 60 (2015) 768–775. https://doi.org/10.1016/j.archoralbio.2015.01.014.
- [11] A. Bigi, E. Boanini, M. Gazzano, Ion substitution in biological and synthetic apatites, in: Biomineralization and Biomaterials, Elsevier, 2016: pp. 235–266. https://doi.org/10.1016/B978-1-78242-338-6.00008-9.
- [12] R.D. Shannon, Revised effective ionic radii and systematic studies of interatomic distances in halides and chalcogenides, Acta Cryst A 32 (1976) 751–767. https://doi.org/10.1107/S0567739476001551.
- [13] S. Peroos, Z. Du, N.H. De Leeuw, A computer modelling study of the uptake, structure and distribution of carbonate defects in hydroxy-apatite, Biomaterials 27 (2006) 2150–2161. https://doi.org/10.1016/j.biomaterials.2005.09.025.
- [14] O.F. Yasar, W.-C. Liao, R. Mathew, Y. Yu, B. Stevensson, Y. Liu, Z. Shen, M. Edén, The Carbonate and Sodium Environments in Precipitated and Biomimetic Calcium Hydroxy-Carbonate Apatite Contrasted with Bone Mineral: Structural Insights from Solid-State NMR, The Journal of Physical Chemistry C 125 (2021) 10572–10592. https://doi.org/10.1021/ACS.JPCC.0C11389.

- [15] C.H. Yoder, M.M. Bollmeyer, K.R. Stepien, R.N. Dudrick, The effect of incorporated carbonate and sodium on the IR spectra of A- and AB-type carbonated apatites, American Mineralogist 104 (2019) 869–877. https://doi.org/10.2138/am-2019-6800.
- [16] E.A.P. De Maeyer, R.M.H. Verbeeck, Possible Substitution Mechanisms for Sodium and Carbonate in Calciumhydroxyapatite, Bulletin Des Sociétés Chimiques Belges 102 (1993) 601–609. https://doi.org/10.1002/bscb.19931020907.
- [17] F.C.M. Driessens, R.M.H. Verbeeck, H.J.M. Heijligers, Some physical properties of Na- and CO3-containing apatites synthesized at high temperatures, Inorganica Chimica Acta 80 (1983) 19–23. https://doi.org/10.1016/S0020-1693(00)91256-8.
- [18] S. Kannan, J.M.G. Ventura, J.M.F. Ferreira, Synthesis and thermal stability of potassium substituted hydroxyapatites and hydroxyapatite/β-tricalciumphosphate mixtures, Ceramics International 33 (2007) 1489–1494. https://doi.org/10.1016/j.ceramint.2006.05.016.
- [19] D.R. Simpson, Substitutions in apatite: I. Potassium-bearing apatite, The American Mineralogist 53 (1968) 432–444.
- [20] R.M.H. Verbeeck, E.A.P. De Maeyer, F.C.M. Driessens, Stoichiometry of Potassium- and Carbonate-Containing Apatites Synthesized by Solid State Reactions, Inorganic Chemistry 34 (1995) 2084– 2088. https://doi.org/10.1021/ic00112a021.
- [21] D. A. Nowicki, J.M. S. Skakle, I. R. Gibson, Potassium—carbonate co-substituted hydroxyapatite compositions: maximising the level of carbonate uptake for potential CO 2 utilisation options, Materials Advances 3 (2022) 1713–1728. https://doi.org/10.1039/D1MA00676B.
- [22] S.L. Wong, C. Drouet, A. Deymier, Carbonate environment changes with Na or K substitution in biomimetic apatites, Materialia 29 (2023) 101795. https://doi.org/10.1016/j.mtla.2023.101795.
- [23] T. Kono, T. Sakae, H. Nakada, T. Kaneda, H. Okada, Confusion between Carbonate Apatite and Biological Apatite (Carbonated Hydroxyapatite) in Bone and Teeth, Minerals 12 (2022) 170. https://doi.org/10.3390/min12020170.
- [24] C. Combes, S. Cazalbou, C. Rey, Apatite biominerals, Minerals 6 (2016) 34. https://doi.org/10.3390/min6020034.
- [25] M.E. Fleet, X. Liu, Carbonate in Synthetic and Biological Apatites, n.d.
- [26] Y. Pan, M.E. Fleet, Compositions of the Apatite-Group Minerals: Substitution Mechanisms and Controlling Factors, Reviews in Mineralogy and Geochemistry 48 (2002) 13–49. https://doi.org/10.2138/rmg.2002.48.2.
- [27] D. Eichert, C. Combes, C. Drouet, C. Rey, Formation and Evolution of Hydrated Surface Layers of Apatites, Key Engineering Materials 284–286 (2005) 3–6. https://doi.org/10.4028/www.scientific.net/kem.284-286.3.
- [28] H. Madupalli, B. Pavan, M.M.J. Tecklenburg, Carbonate substitution in the mineral component of bone: Discriminating the structural changes, simultaneously imposed by carbonate in A and B sites of apatite, Journal of Solid State Chemistry 255 (2017) 27–35. https://doi.org/10.1016/j.jssc.2017.07.025.
- [29] A.C. Deymier, A.K. Nair, B. Depalle, Z. Qin, K. Arcot, C. Drouet, C.H. Yoder, M.J. Buehler, S. Thomopoulos, G.M. Genin, J.D. Pasteris, Protein-free formation of bone-like apatite: New insights into the key role of carbonation, Biomaterials 127 (2017) 75–88. https://doi.org/10.1016/j.biomaterials.2017.02.029.
- [30] R.Z. Legeros, O.R. Trautz, J.P. Legeros, E. Klein, W.P. Shirra, Apatite Crystallites: Effects of Carbonate on Morphology, Science 155 (1967) 1409–1411. https://doi.org/10.1126/science.155.3768.1409.
- [31] A.A. Baig, J.L. Fox, J. Hsu, Z. Wang, M. Otsuka, W.I. Higuchi, R.Z. LeGeros, Effect of Carbonate Content and Crystallinity on the Metastable Equilibrium Solubility Behavior of Carbonated Apatites, Journal of Colloid and Interface Science 179 (1996) 608–617. https://doi.org/10.1006/jcis.1996.0255.

- [32] A.A. Baig, J.L. Fox, R.A. Young, Z. Wang, J. Hsu, W.I. Higuchi, A. Chhettry, H. Zhuang, M. Otsuka, Relationships among carbonated apatite solubility, crystallite size, and microstrain parameters, Calcified Tissue International 64 (1999) 437–449. https://doi.org/10.1007/PL00005826.
- [33] B. Wingender, M. Azuma, C. Krywka, P. Zaslansky, J. Boyle, A.C. Deymier, Carbonate substitution significantly affects the structure and mechanics of carbonated apatites, Acta Biomaterialia (2020).
- [34] G.H. Nancollas, B. Tomazic, Growth of calcium phosphate on hydroxyapatite crystals. Effect of supersaturation and ionic medium, Journal of Physical Chemistry 78 (1974) 2218–2225. https://doi.org/10.1021/j100615a007.
- [35] C.J.S. Ibsen, H. Leemreize, B.F. Mikladal, J. Skovgaard, M. Bremholm, J.R. Eltzholtz, B.B. Iversen, H. Birkedal, Alkali Counterions Impact Crystallization Kinetics of Apatite Nanocrystals from Amorphous Calcium Phosphate in Water at High pH, Crystal Growth and Design 18 (2018) 6723–6728. https://doi.org/10.1021/acs.cgd.8b01008.
- [36] M.E. Fleet, Infrared spectra of carbonate apatites: Evidence for a connection between bone mineral and body fluids, American Mineralogist 102 (2017) 149–157. https://doi.org/10.2138/am-2017-5704
- [37] M.S. Sader, K. Lewis, G.A. Soares, R.Z. Legeros, Simultaneous Incorporation of Magnesium and Carbonate in Apatite: Effect on Physico-chemical Properties, (2013). https://doi.org/10.1590/S1516-14392013005000046.
- [38] R.Z. LeGeros, T. Sakae, C. Bautista, M. Retino, J.P. LeGeros, Magnesium and carbonate in enamel and synthetic apatites., Advances in Dental Research 10 (1996) 225–231. https://doi.org/10.1177/08959374960100021801.
- [39] A. Joseph Nathanael, D. Mangalaraj, S.I. Hong, Y. Masuda, Y.H. Rhee, H.W. Kim, A.J. Nathanael, D. Mangalaraj, S.I. Hong, Y. Masuda, Y.H. Rhee, H.W. Kim, Influence of fluorine substitution on the morphology and structure of hydroxyapatite nanocrystals prepared by hydrothermal method, Materials Chemistry and Physics 137 (2013) 967–976. https://doi.org/10.1016/j.matchemphys.2012.11.010.
- [40] M. Crisostomo, C. Ureta, Salivary pH and Taste Sensitivity among Geriatric and Non-Geriatric Patients in a Tertiary Hospital: A Cross Sectional Study, Philippine Journal of Otolaryngology Head and Neck Surgery 34 (2019) 11–15. https://doi.org/10.32412/pjohns.v34i2.125.
- [41] M.J. Larsen, A.F. Jensen, D.M. Madsen, E.I.F. Pearce, Individual variations of pH, buffer capacity, and concentrations of calcium and phosphate in unstimulated whole saliva, Archives of Oral Biology 44 (1999) 111–117. https://doi.org/10.1016/S0003-9969(98)00108-3.
- [42] and M.C.H. van der M. Eve Donnelly, Adele L. Boskey, Shefford P. Baker, Effects of tissue age on bone tissue material composition and nanomechanical properties in the rat cortex, Journal of Biomedical Materials Research Part A 92 (2010) 1048–1056. https://doi.org/10.1161/CIRCULATIONAHA.110.956839.
- [43] P.G. Spizzirri, N.J. Cochrane, S. Prawer, E.C. Reynolds, A Comparative Study of Carbonate Determination in Human Teeth Using Raman Spectroscopy, Caries Research 46 (2012) 353–360. https://doi.org/10.1159/000337398.
- [44] M.M. Moynahan, S.L. Wong, A.C. Deymier, Beyond dissolution: Xerostomia rinses affect composition and structure of biomimetic dental mineral in vitro, PLoS ONE 16 (2021) 5–7. https://doi.org/10.1371/journal.pone.0250822.
- [45] S.M. Barinov, I.V. Fadeeva, D. Ferro, J.V. Rau, S.N. Cesaro, V.S. Komlev, A.S. Fomin, Stabilization of Carbonate Hydroxyapatite by Isomorphic Substitutions of Sodium for Calcium, Russ. J. Inorg. Chem. 53 (2008) 164–168. https://doi.org/10.1134/S0036023608020022.
- [46] Z. Zyman, M. Tkachenko, Sodium-carbonate co-substituted hydroxyapatite ceramics, PAC 7 (2013) 153–157. https://doi.org/10.2298/PAC1304153Z.

- [47] D.A. Bushinsky, N.S. Krieger, Effects of acid on bone, Kidney International 101 (2022) 1160–1170. https://doi.org/10.1016/j.kint.2022.02.032.
- [48] N.S. Krieger, K.K. Frick, D.A. Bushinsky, Mechanism of acid-induced bone resorption, Current Opinion in Nephrology and Hypertension 13 (2004) 423–436. https://doi.org/10.1097/01.mnh.0000133975.32559.6b.
- [49] S.L. Wong, A.C. Deymier, Phosphate and buffer capacity effects on biomimetic carbonate apatite, Ceramics International 49 (2023) 12415–12422. https://doi.org/10.1016/j.ceramint.2022.12.101.
- [50] J.F. Ferguson, P.L. McCarty, Effects of carbonate and magnesium on calcium phosphate precipitation, Environ. Sci. Technol. 5 (1971) 534–540. https://doi.org/10.1021/es60053a005.
- [51] X. Cao, W. Harris, Carbonate and Magnesium Interactive Effect on Calcium Phosphate Precipitation, Environ. Sci. Technol. 42 (2008) 436–442. https://doi.org/10.1021/es0716709.
- [52] J. Ha, S.-A. Kim, K. Lim, S. Shin, The association of potassium intake with bone mineral density and the prevalence of osteoporosis among older Korean adults, Nutr Res Pract 14 (2020) 55–61. https://doi.org/10.4162/nrp.2020.14.1.55.
- [53] J. Green, C.R. Kleeman, Role of bone in regulation of systemic acid-base balance, Kidney International 39 (1991) 9–26. https://doi.org/10.1038/ki.1991.2.
- [54] J. Lemann, D.A. Bushinsky, L.L. Hamm, Bone buffering of acid and base in humans, American Journal of Physiology Renal Physiology 285 (2003). https://doi.org/10.1152/ajprenal.00115.2003.
- [55] S. Von Euw, Y. Wang, G. Laurent, C. Drouet, F. Babonneau, N. Nassif, T. Azaïs, Bone mineral: new insights into its chemical composition, Scientific Reports 9 (2019) 1–11. https://doi.org/10.1038/s41598-019-44620-6.
- [56] C. Combes, C. Rey, S. Mounic, Identification and evaluation of HPO4 ions in biomimetic poorly crystalline apatite and bone mineral, Key Engineering Materials 192–195 (2001) 143–146.
- [57] C. Drouet, M. Aufray, S. Rollin-Martinet, N. Vandecandelaère, D. Grossin, F. Rossignol, E. Champion, A. Navrotsky, C. Rey, Nanocrystalline apatites: The fundamental role of water, American Mineralogist 103 (2018) 550–564. https://doi.org/10.2138/am-2018-6415.
- [58] M.A. Brown, G.V. Bossa, S. May, Emergence of a Stern Layer from the Incorporation of Hydration Interactions into the Gouy–Chapman Model of the Electrical Double Layer, Langmuir 31 (2015) 11477–11483. https://doi.org/10.1021/acs.langmuir.5b02389.
- [59] I. Siretanu, D. Ebeling, M.P. Andersson, S.L.S. Stipp, A. Philipse, M.C. Stuart, D. Van Den Ende, F. Mugele, Direct observation of ionic structure at solid-liquid interfaces: a deep look into the Stern Layer, Sci Rep 4 (2014) 4956. https://doi.org/10.1038/srep04956.
- [60] N.X. West, J.A. Hughes, M. Addy, The effect of pH on the erosion of dentine and enamel by dietary acids in vitro, Journal of Oral Rehabilitation 28 (2008) 860–864. https://doi.org/10.1111/j.1365-2842.2001.00778.x.
- [61] S. Shimabayashi, M. Matsumoto, Non-stoichiometric Dissolution of Hydroxyapatite in the Presence of Simple Salts, Nippon Kagaku Kaishi 1993 (1993) 1118–1122. https://doi.org/10.1246/nikkashi.1993.1118.
- [62] S. Habelitz, G.W. Marshall, M. Balooch, S.J. Marshall, Nanoindentation and storage of teeth, Journal of Biomechanics 35 (2002) 995–998. https://doi.org/10.1016/S0021-9290(02)00039-8.
- [63] S.E. Strawn, J.M. White, G.W. Marshall, L. Gee, H.E. Goodis, S.J. Marshall, Spectroscopic changes in human dentine exposed to various storage solutions short term, Journal of Dentistry 24 (1996) 417–423. https://doi.org/10.1016/0300-5712(95)00106-9.

## Presence of $K^{\scriptscriptstyle +}$ in solution acts as a protectant against dissolution of biomimetic apatites compared to $Na^{\scriptscriptstyle +}$

Authors: Stephanie Wong<sup>1</sup>, Katherine R. Peccerillo<sup>2</sup>, Margaret Easson<sup>3</sup>, Trey Doktorski<sup>3</sup>, Alix C. Deymier<sup>1,3\*</sup>

- 1. Dept of Biomedical Engineering, University of Connecticut Health Center, Farmington, CT
- 2. School of Dental Medicine, University of Connecticut Health Center, Farmington, CT
- 3. Dept of Biomedical Engineering, University of Connecticut, Storrs, CT

## \*Corresponding Author:

Email: deymier@uchc.edu

Alix Deymier
Dept of Biomedical Engineering
School of Dental Medicine
University of Connecticut Health Center
263 Farmington Ave
Farmington, CT 06030
Phone: 1-520-248-1956

## **Abstract**

Tooth mineral is constantly exposed to saliva. Based on many factors including diet and chronic disease, salivary composition can vary in pH and potassium (K<sup>+</sup>) and sodium (Na<sup>+</sup>) concentrations. Tooth mineral is composed of bioapatite with an ability for ionic exchange between the mineral and the surrounding fluid. Na<sup>+</sup> and K<sup>+</sup> are known to integrate into biomimetic apatites during crystallization and affect crystallization growth/rate and morphology of calcium phosphates. However, it is unknown how exogenous Na<sup>+</sup> and K<sup>+</sup> in the solution affect carbonated apatite after formation. Therefore, we investigated the mechanistic differences between Na<sup>+</sup> and K<sup>+</sup> on biomimetic apatite dissolution/recrystallization. To do so, biomimetic carbonated apatites with 3 or 7 wt% CO<sub>3</sub><sup>2</sup> were exposed to NaCl or KCl solutions at various concentrations and pHs seen in saliva. Powder mass, Raman, FTIR, and XRD were used to determine the weight, composition, and structure of the mineral while the solution was characterized for pH and ionic variations. After mineral-solution exposure, significant differences were seen between NaCl and KCl solutions. The apatites exposed to NaCl underwent a classical dissolution/recrystallization mechanism exhibiting more loss in mass and carbonate during dissolution with modifications of A-, B-, and labile CO<sub>3</sub><sup>2-</sup> amounts during recrystallization which were dependent on the initial apatite CO<sub>3</sub><sup>2</sup>- content. Meanwhile, apatites exposed to KCl had less mass loss during dissolution and retained the crystal structure, A-, B-, and labile CO<sub>3</sub><sup>2</sup>amounts during recrystallization, suggesting that K<sup>+</sup> may shield apatites from dissolution. To our knowledge, this is the first study to parse out mechanistic differences between Na<sup>+</sup> and K<sup>+</sup> on biomimetic carbonated apatite dissolution/recrystallization. Overall, this study will provide insight on how fluctuating Na<sup>+</sup> and K<sup>+</sup> in saliva may affect tooth mineral composition and structure.

Keywords: B Spectroscopy, C Chemical properties, D Apatite, E Biomedical Applications, B Impurities

## 1. Introduction

Teeth are continuously bathed in saliva. Saliva is a complex fluid with an ever-changing composition. These changes depend on many factors, including time of day, stress [1], diet [2,3], and health conditions such as hyposalivation [4], aging [5], diabetes [6], and chronic kidney disease [7]. Two of the primary ionic components in saliva are sodium (Na<sup>+</sup>) and potassium (K<sup>+</sup>). These can fluctuate in concentration between 11.5-271.9 mM and 2.6-27.4 mM, respectively[1–7]. The changes in salivary ionic composition give way to modified ionic exchange mechanisms between the surrounding saliva and tooth mineral [8].

Enamel and dentin are primarily composed of calcium-deficient carbonate-substituted apatite mineral [8–10]. This mineral is known for allowing substitutional ionic exchanges within its structure [11]. Some of these include cationic substitutions of Na<sup>+</sup> and K<sup>+</sup>. Na<sup>+</sup> can easily substitute for calcium (Ca<sup>2+</sup>) due to its similar ionic sizes (1.02 for Na<sup>+</sup> vs 1.00 for Ca<sup>2+</sup> for ionic radii size [12,13]. On the other hand, K<sup>+</sup> has more difficulty substituting into the mineral lattice for Ca<sup>2+</sup> due to its larger ionic radius (1.38) [13]. Since these monovalent ions substitute for the divalent Ca<sup>2+</sup> ion. Na<sup>+</sup> and K<sup>+</sup> must be co-substituted with another ion, typically carbonate (CO<sub>3</sub><sup>2-</sup> ), to maintain charge balance [13]. For Na and CO<sub>3</sub><sup>2</sup>-coupled substitutions, previous studies have extensively identified the molecular interactions between Na<sup>+</sup> and CO<sub>3</sub><sup>2-</sup> with most studies concluding the importance of Na<sup>+</sup> within the apatite structure [14–17]. Other studies have also identified K<sup>+</sup> sole effect on the apatites structure [18,19], albeit to a lesser extent, with little information about its coupled substitution with CO<sub>3</sub><sup>2-</sup> compared to Na<sup>+</sup> [20,21]. Recently, our lab discovered that co-substitutions of Na<sup>+</sup> or K<sup>+</sup> with CO<sub>3</sub><sup>2-</sup> modifies the location of the CO<sub>3</sub><sup>2-</sup> within the apatite lattice, such as increased A-type CO<sub>3</sub><sup>2-</sup> in apatites synthesized with K<sup>+</sup> compared to Na<sup>+</sup> [22]. This resulted in modifications to the mineral structure and physiochemical properties.

CO<sub>3</sub><sup>2-</sup> substitution is one of the most common anionic substitutions in enamel and dentin. Enamel contains about 2 wt% CO<sub>3</sub><sup>2-</sup>, while dentin has ~5-7 wt% CO<sub>3</sub><sup>2-</sup> [8,9,23]. These carbonate ions can substitute in multiple places within the apatite structure. Carbonate can exchange for phosphate, known as B-type CO<sub>3</sub><sup>2-</sup>, and/or for the hydroxyl groups, known as A-type CO<sub>3</sub><sup>2-</sup>, within the crystalline core [24–26]. Carbonate can also reside in the amorphous hydrated layer, known as labile CO<sub>3</sub><sup>2-</sup> [24,27]. Changes in CO<sub>3</sub><sup>2-</sup> content and location can modify the morphological, structural, and chemical characteristics of apatite [25,28–30]. For example, increased B-type CO<sub>3</sub><sup>2-</sup> substitutions increase the mineral solubility and decrease the crystallinity [29,31], crystallite size [31,32] and stiffness [33]. Additionally, these substitutions change the atomic lattice spacing along both the a- and c-axes [28,29]. As it has previously been shown that Na<sup>+</sup> and K<sup>+</sup> can modify CO<sub>3</sub><sup>2-</sup> co-substitutions within the apatite lattice, this suggests that substitutions of Na<sup>+</sup> and K<sup>+</sup> that affect CO<sub>3</sub><sup>2-</sup> locations and concentrations could have significant effects on the solubility, structure, and mechanics of tooth minerals.

In addition to its effect on CO<sub>3</sub><sup>2-</sup>, Na<sup>+</sup> and K<sup>+</sup> have also been shown to affect the crystallization and growth of calcium phosphates. For example, previous studies have shown that NaCl and KCl solutions have distinct differences on calcium phosphate crystal growth [34], nucleation rate [35], and crystal shape [35]. In addition, Na<sup>+</sup> incorporation during crystallization

affects physiochemical properties of apatite, such as  $CO_3^{2-}$  vibrations [15,36]. Despite knowing that  $Na^+$  and  $K^+$  can affect mineral growth, structure, and composition - much like other ionic components such as  $Mg^+$  and  $F^-$  [37–39] - it is unknown how they affect biomimetic carbonated apatites after formation. Therefore, the goal of this study was to determine how extant biomimetic carbonated apatite is altered during exposure to  $Na^+$  and  $K^+$ -rich solutions that simulate the concentrations range of  $Na^+$  and  $K^+$  within saliva. This study will provide insight as to how tooth mineral may react during salivary variations in  $Na^+$  or  $K^+$  content.

## 2. Methods

## 2.1. Synthesis

To mimic the carbonate content in enamel and dentin, biomimetic apatite powders were synthesized through an aqueous precipitation reaction with an aim to obtain ~3 and ~7 wt% carbonate as previously described [29]. In short, 50 mL of 0.15 M calcium nitrate tetrahydrate (ACROS, USA), 50 mL of 0.09 M sodium phosphate (ACROS, India) were slowly titrated drop by drop into a 250 mL of either 0 mM or 6 mM sodium bicarbonate (Sigma-Aldrich, France) for 3 or 7 wt% CO<sub>3</sub><sup>2-</sup> substitution, respectively, at 60°C. The low and high wt% of CO<sub>3</sub><sup>2-</sup> represents enamel and dentin, respectively. The pH was maintained at ~pH 9 with 0.1 M NaOH (ACROS, Sweden). Once completely titrated, the mixture was left to mature for 2 hours at ~pH 9 at 60°C. Afterwards, the precipitate was filtered, rinsed thoroughly, and dried at 60°C overnight. X-Ray Diffraction and Raman Spectroscopy was used to confirm the apatitic phase with carbonate substitutions. The amount of carbonate was determined by comparing the carbonate to phosphate ratio to our standardized carbonate apatites that were correlated to the carbon amount determined by Carbon Hydrogen Nitrogen [29].

## 2.2. Dissolution/exposure experiment

50 mg of apatite with either 3% or 7% substituted carbonate was placed into 10 mL of either sodium chloride or potassium chloride in conical tubes. 3 concentrations of sodium chloride (Fisher, USA) or potassium chloride (Sigma-Aldrich, USA) were used: 0.05 M, 0.1 M, 0.2 M, at 2 different pH's, pH 5.5 and pH 7.4 (Supplemental Figure 1) to represent low and high amounts of Na<sup>+</sup> or K<sup>+</sup> concentrations at acidic and neutral pH's that can occur in the mouth [40,41]. The powders were exposed to the solutions for 3 days and the pH of the solutions were obtained at 1, 3, 6, 24, 48, and 72 hours. After 3 days, the powders were filtered with P4 filter paper (Fisher Scientific, China), rinsed with 10 mL of Millipore water 3 times, and dried at 60°C overnight. The powders were massed to determine the mass lost during the exposure period. Each condition had 3 replicates.

## 2.3. Raman Spectroscopy

The composition of the powders was initially determined by using Raman spectroscopy. Using a WiTec alpha300 with a 785 nm laser, 10 points per sample were obtained at an acquisition time of 1 second for 30 accumulations. The following peaks were fit using the Lorentzian fit function of WiTec Program 5.1 to obtain the following peak areas:  $v_3 PO_4^{3-}$  (430 cm<sup>-1</sup>),  $v_4 PO_4^{3-}$  (590 cm<sup>-1</sup>),  $v_1 PO_4^{3-}$  (950 cm<sup>-1</sup>),  $v_1 PO_4^{3-}$  (960 cm<sup>-1</sup>),  $v_2 PO_4^{3-}$  (1050 cm<sup>-1</sup>), and  $v_1 CO_3^{2-}$  (1070 cm<sup>-1</sup>). The carbonate to phosphate ratio ( $CO_3/PO_4$ ) was calculated from the ratio of

the 1070/(950+960) peak areas for each sample to determine the percent change in  $CO_3/PO_4$  (% $\Delta$   $CO_3/PO_4$ ) [29,42,43]. Each condition had 3 replicates.

## 2.4. Fourier Transform Infrared Spectroscopy

Attenuated Total Reflectance (ATR) FTIR spectroscopy was used to confirm the apatite characteristic phase and determine the amount of A-type, B-type, and labile CO<sub>3</sub><sup>2-</sup> in the apatites before and after exposure. Using a Nicolet Magna-IR 500 spectrometer, each powder had an acquisition of 64 scans with a resolution of 2 cm<sup>-1</sup> from 400-4000 cm<sup>-1</sup>. Using the OriginPro 2021b software (OriginLab Corporation, Northampton, MA, USA), the v<sub>2</sub> CO<sub>3</sub><sup>2-</sup> peak within the 900-750 cm<sup>-1</sup> range were deconvoluted for the A-type, B-type, and labile CO<sub>3</sub><sup>2-</sup> peaks with the respective initial peak centers of 880 cm<sup>-1</sup>, 873 cm<sup>-1</sup>, 867 cm<sup>-1</sup> using a Gaussian fit function [15]. Each condition had 3 replicates.

## 2.5. X-Ray Diffraction

The structure and phase of the powders were determined by X-ray Diffraction. Each sample was analyzed from 20-60° 20 with 0.02° step with 1 second per step using a Bruker D2 Phaser Diffractometer (Bruker AXS, Germany) operating at 30 kV and 10 mA. 11 peaks were deconvoluted using a PseudoVoigt function with the Diffrac.Eva software to determine the peak centers, full width at half max (FWHM), crystallite length and width, and lattice spacing of the apatites before and after solution exposure. The d-spacing for the 002, 310, and 004 planes were scrutinized. Afterwards, the crystallite length and width determined by the 002 and 310 planes respectively were determined via Scherrer's equation using the peak FWHM. The powders were compared against stoichiometric hydroxyapatite from the Powder Diffraction File from the International Centre for Diffraction Data (ICDD). Each condition had 3 replicates.

## 2.6. Inductively Coupled Plasma – Optical Emission Spectroscopy (ICPOES)

One solution sample from each condition (n=1) was analyzed for changes in calcium (Ca), phosphorus (P), sodium (Na), and potassium (K) before and after solution exposure via a Perkin Elmer 7300DV Dual View Inductively Coupled Plasma–Optical Emission Spectrometer (ICP-OES). All samples were directly analyzed at 20x dilution due to the very high levels of phosphate in the samples. Standard quality assurance procedures were employed, including analysis of initial and continuing calibration checks and blanks, duplicate samples, preparation blanks (Blank), post digestion spiked samples, and laboratory control samples (LCS).

## 2.7. Statistical Analyses

Multiway Analysis of Variance (ANOVA) with Tukey test comparison was used in OriginPro 2021b (OriginLab Corporation, Northampton, MA, USA) to determine the statistical significance for the aforementioned quantitative analyses and between the independent variables of pH, concentration,  $Na^+$  vs  $K^+$ , and wt%  $CO_3^{2-}$ . Significance is classified as p<0.05.

## 3. Results

## 3.1. pH

The change in solution pH ( $\Delta$ pH) with mineral exposure was significantly higher when the solution had an initial pH of 5.5 (pH<sub>i</sub> 5.5) compared to pH<sub>i</sub> 7.4 (Figure 1A and Supplemental

Table 1). The average  $\Delta pH$  was between 1.48 and 2.49 for the 3%  $CO_3^{2-}$  apatites at  $pH_i$  5.5 and between 1.81 and 3.02 for 7%  $CO_3^{2-}$  apatites at  $pH_i$  5.5. This is 15X larger than the average  $\Delta pH$  for  $pH_i$  7.4 which ranged from -0.12 to 0.20 for 3%  $CO_3^{2-}$  and -0.13 to 0.92 for 7%  $CO_3^{2-}$ .

Regarding the solution cationic concentration, the increase in [Na<sup>+</sup>] or [K<sup>+</sup>] molar concentrations generally decreased the  $\Delta pH$  overall at all pH's and wt%  $CO_3^{2^-}$ . However, the differences were only statistically significant for 0.05 M concentrations for both Na<sup>+</sup> and K<sup>+</sup> when considering pH and wt%  $CO_3^{2^-}$  as factors (Supplemental Table 2).  $\Delta pH$  of the solution when mineral was added to water was the lowest value in nearly all cases, contrary to the trend suggesting that increased cationic content reduced  $\Delta pH$ .

When comparing crystals containing either 3% or 7% substituted  $CO_3^{2-}$  at all conditions, the 7%  $CO_3^{2-}$  samples induced a significantly larger  $\Delta pH$  in all solutions compared to their 3%  $CO_3^{2-}$  counterparts (Supplemental Table 3). Similarly, when comparing the effect of KCl versus NaCl, the KCl solutions exhibited a significantly larger  $\Delta pH$  than their NaCl and water counterparts when factoring wt%  $CO_3^{2-}$  and pH (Supplemental Table 4). Conversely, there was no significant difference between NaCl and water.

### 3.2. Mass

KCl had significantly less mineral mass lost after exposure than NaCl at both 3% and 7%  $\rm CO_3^{2-}$  (Figure 1B and Supplemental Tables 5-6). For 3%  $\rm CO_3^{2-}$ , there's roughly 20% more mass loss in NaCl than KCl, while NaCl had 40-50% more mass loss than KCl at 7%  $\rm CO_3^{2-}$ . There were no apparent trends with concentration or pH in mass lost. However, more mass was lost at 3%  $\rm CO_3^{2-}$  than 7% for KCl as well as NaCl (Supplemental Tables 7-8).

## 3.3. Raman – Carbonate content

Overall, the % $\Delta$ CO3/PO4 was significantly higher for the mineral placed in KCl than in NaCl at 3 wt% CO<sub>3</sub><sup>2-</sup>, indicating higher amounts of CO<sub>3</sub><sup>2-</sup> in the mineral in KCl (Figure 2 and Supplemental Table 9). For NaCl solution exposures, the % $\Delta$ CO3/PO4 was generally unchanged at pH 5.5 for apatites with an initial 3% and 7% CO<sub>3</sub><sup>2-</sup> substitution. However, the % $\Delta$ CO3/PO4 was significantly elevated for crystals containing 3% CO<sub>3</sub><sup>2-</sup> compared to 7% CO<sub>3</sub><sup>2-</sup> at pH 7.4 (Supplemental Table 10). For the mineral exposed to KCl, the % $\Delta$ CO3/PO4 significantly increased about ~20-30% at both pHs and at all concentrations for 3 wt% CO<sub>3</sub><sup>2-</sup> compared to 7% CO<sub>3</sub><sup>2-</sup> (Supplemental Table 11).

## 3.4. FTIR - Carbonate type

Raman established that the apatite crystals placed in KCl had higher CO<sub>3</sub><sup>2-</sup> content than apatite placed in NaCl especially for crystals with low starting CO<sub>3</sub><sup>2-</sup> (3%). FTIR data indicates that this may be due to shifts in the CO<sub>3</sub><sup>2-</sup> environment within the crystal lattice. For 3 wt% CO<sub>3</sub><sup>2-</sup> for apatites exposed to all solutions, the relative amounts of A-type CO<sub>3</sub><sup>2-</sup> generally did not change after being exposed to all pH's and concentrations (Figure 3A). At an initial 7 wt% CO<sub>3</sub><sup>2-</sup> content, the amount of A-type CO<sub>3</sub><sup>2-</sup> generally decreased for apatites exposed to NaCl at all concentrations and pHs compared to the unexposed powder (Ctrl); however, no apparent trends in terms of concentrations nor pH were observed. For apatites with an initial 7 wt% CO<sub>3</sub><sup>2-</sup>, there

were no changes in  $CO_3^{2-}$  content as a function of  $CO_3^{2-}$  location. In addition, there were no changes in A-type  $CO_3^{2-}$  between the 3% and 7%  $CO_3^{2-}$  unexposed control groups.

The 7 wt%  $CO_3^{2-}$  unexposed control had higher levels of B-type  $CO_3^{2-}$  compared to the 3 wt% control as expected (Figure 3B). For 3 wt%  $CO_3^{2-}$ , apatites placed in water generally increased in B-type  $CO_3^{2-}$  at both pH's. At the same  $CO_3^{2-}$  content, apatites exposed to NaCl showed a decreasing trend in B-type  $CO_3^{2-}$  compared to controls at both pH's, while apatites in KCl retained the same amount of B-type  $CO_3^{2-}$  at all concentrations and pH's except 0.05 M KCl at pH 5.5. Three wt%  $CO_3^{2-}$  apatites placed in NaCl exhibited less B-type  $CO_3^{2-}$  than those in KCl. For apatites with an initial 7 wt%  $CO_3^{2-}$ , there were no changes or trends in B-type content after exposure for all solutions, concentrations, and pHs.

For the unexposed samples (Ctrl), the relative amounts of labile  ${\rm CO_3}^{2-}$  decreased as the initial wt%  ${\rm CO_3}^{2-}$  increased (Figure 3C). At 3 wt%  ${\rm CO_3}^{2-}$ , apatites exposed to NaCl showed a trending increase in labile  ${\rm CO_3}^{2-}$  compared to the unexposed control sample while KCl samples generally showed no changes and water samples showed a trending decrease in labile  ${\rm CO_3}^{2-}$ . Contrarily, there were no changes in labile  ${\rm CO_3}^{2-}$  at 7 wt%  ${\rm CO_3}^{2-}$  after exposure to all conditions.

#### 3.5. XRD – Structure

The apatites before exposure to the solutions exhibited an average d-spacing of 3.445 and 3.444 along the 002 (c-axis) for 3 and 7 wt% CO<sub>3</sub><sup>2-</sup>, respectively, while the average 310 (a-axis) d-spacing was 2.273 and 2.264 (Figure 4A-B). The increased c-axis spacing and the decreased a-axis between the initial 3% and 7% CO<sub>3</sub><sup>2-</sup> apatites agrees with previously reported trends for B-type apatites [29]. For 3 wt% CO<sub>3</sub><sup>2-</sup> apatites exposed to NaCl, the c-axis and a-axis showed a trending decrease compared to the unexposed control apatite at pH 7.4. However, there were no statistically significant differences in the mineral c-axis or a-axis spacing as a function of any of the independent variables.

For crystallite size, 3% CO<sub>3</sub><sup>2-</sup> had a significantly higher crystallite length and width along the c-axis and a-axis, respectively, compared to 7% CO<sub>3</sub><sup>2-</sup> for all variables as expected (Figure 5A-B and Supplemental Tables 12-13) [29,44]. 3% CO<sub>3</sub><sup>2-</sup> apatite at all conditions had between 230.04-321.72 nm in crystallite length with no significant changes between conditions. 7% CO<sub>3</sub><sup>2-</sup> apatite in all conditions had between 106.30-189.09 nm in crystallite length (Figure 5A) with no significance between changes as well. Additionally, NaCl exhibited a trend of higher crystallite length than KCl, specifically at pH 7.4 at all wt% CO<sub>3</sub><sup>2-</sup> as well as 7% CO<sub>3</sub><sup>2-</sup> at pH 5.5. There were no trends with concentration or pH at either wt% CO<sub>3</sub><sup>2-</sup> or within NaCl and KCl.

The crystallite width for 3 wt%  $CO_3^{2-}$  apatites exposed to water increased in water at pH 5.5 and 7.4 (Figure 5B). The crystallite width also increased for 3 wt%  $CO_3^{2-}$  in NaCl at pH 7.4 as compared to unexposed control while the width either stayed the same or decreased in KCl. For apatites with an initial 7 wt%  $CO_3^{2-}$ , no changes were observed for apatites exposed to water and KCl. Contrarily, the width significantly increased for all NaCl conditions compared to KCl (Supplemental Table 14).

## 3.6. ICP-OES – Ionic content of solutions

The solutions before and after exposure to the apatite powders were analyzed for  $Ca^{2+}$ , P,  $Na^+$ , and  $K^+$  content through ICP-OES to determine the change of solutes ( $\Delta Ca$ ,  $\Delta P$ ,  $\Delta Na$ , and  $\Delta K$ ).  $\Delta Ca$  and  $\Delta P$  increased in the solution at all conditions for 3 and 7 wt%  $CO_3^{2-}$ , indicating an increase of  $Ca^{2+}$  and P after exposure to the apatite powders (Figure 6A-B). While 3%  $CO_3^{2-}$  apatites were generally similar in  $Ca^{2+}$  and P content in the solution after exposure to the powders, 7 wt%  $CO_3^{2-}$  apatites in NaCl at pH 5.5 as well as water at both pH's had an increased  $Ca^{2+}$  and P content in the solution compared to NaCl pH 7.4 and KCl at all conditions. There were generally no significant changes between KCl at all conditions at 7 wt%  $CO_3^{2-}$ .

As expected,  $\Delta$ Na content did not change in the solution for water and KCl for 3 and 7 wt%  $CO_3^{2-}$  apatites, irrespective of pH and concentration (Figure 6C). Na<sup>+</sup> content in the solution with 7 wt%  $CO_3^{2-}$  generally did not change as well. However, for NaCl solutions with 3%  $CO_3^{2-}$  apatites, the amount of Na<sup>+</sup> in the solution decreased, especially for pH 7.4 with increasing NaCl concentration.

Conversely,  $K^+$  content in the solution did not change for NaCl irrespective of wt%  $CO_3^2$ , concentration, and pH after exposure to the powders as expected (Figure 6D). There were inconsistent changes with KCl, exhibiting a range of either relatively low to high increases or decreases of  $K^+$  content in the solution for both wt%  $CO_3^{2-}$ .

## 4. Discussion

Teeth are mainly composed of dynamic carbonated apatite mineral which is subjected to many ionic fluctuations in the surrounding salivary fluid, such as variations in Na<sup>+</sup> or K<sup>+</sup> concentration. Because the apatite mineral easily allows substitutions to occur, these Na<sup>+</sup> and K<sup>+</sup> ions can integrate, ultimately changing the composition and mineral structure [20,22]. While many previous studies by others and ourselves have determined that Na<sup>+</sup> increases B-type CO<sub>3</sub><sup>2</sup>incorporation into apatites during formation [22,45,46], we recently discovered that K<sup>+</sup> can increase the amount of A-type CO<sub>3</sub><sup>2</sup>- substitution during bone-like apatite synthesis [22]. These different co-substitutions within apatite ultimately changed the lattice structure and carbonate environment despite the lower K<sup>+</sup> incorporation into apatite compared to Na<sup>+</sup>. Previous studies have also shown that NaCl and KCl solutions can affect crystal growth of calcium phosphates differently, in which increased NaCl concentration increased the crystal growth rate compared to KCl [35]. However, the growth rate decreases when seeded crystals were placed in NaCl [34]. While these studies have looked at the effects of Na<sup>+</sup> and K<sup>+</sup> during synthesis, crystallization, and growth, it is important to understand how Na<sup>+</sup> and K<sup>+</sup> in the solution affect pre-existing carbonated apatites after crystallization. In this study, to better understand this behavior, biomimetic apatites with 3 and 7 wt% CO<sub>3</sub><sup>2</sup> were exposed to increasing NaCl or KCl concentrations with either pH 5.5 or 7.4 to represent possible variations in salivary chemistry.

When the apatite crystals were exposed to NaCl solutions, the significant increase in pH, especially at initially low starting pH (pH<sub>i</sub>), was expected as acidic solutions increase apatite dissolution and release larger concentrations of buffering ions, such as  $CO_3^{2-}$  and  $PO_4^{3-}$  (Figure 1) [44,47–49]. Apatite dissolution in NaCl was confirmed by the reduction of crystal mass and

increase of Ca<sup>2+</sup> and P in the solution after exposure for both pHs and initial wt% CO<sub>3</sub><sup>2-</sup> (Figure 6A-B). Along with a loss of mass (Figure 1B), apatite exposed to lower pHs has been associated with decreased mineral CO<sub>3</sub><sup>2-</sup> content [44,49]. Indeed, at low pH<sub>i</sub>, both the 3 and 7% CO<sub>3</sub><sup>2-</sup> apatites exhibit a decrease in CO<sub>3</sub><sup>2-</sup> with exposure, indicating that CO<sub>3</sub><sup>2-</sup> was released from apatite to increase the solution pH (Figure 2). At pH 7.4, the increased or lack of change within the mineral CO<sub>3</sub><sup>2-</sup> content correlates with the lack of change in ΔpH at the elevated pH<sub>i</sub> (Figure 1A). This suggests that less dissolution was occurring for apatites in NaCl at higher pHs, agreeing with previous studies [44]. Together, these results point to a classical dissolution phenomena in NaCl in which the apatite mineral dissolves by releasing buffering ions, specifically CO<sub>3</sub><sup>2-</sup>, to increase the solution pH.

CO<sub>3</sub><sup>2</sup>- can substitute into three separate locations in the apatite mineral crystal and it is unclear which locations are preferentially affected by solution exposure. For apatites in NaCl, the initial crystal composition played an essential role in determining which CO<sub>3</sub><sup>2</sup> was most affected by solution exposure. The general loss of B-type CO<sub>3</sub><sup>2-</sup> for 3 wt% CO<sub>3</sub><sup>2-</sup> apatites in NaCl for all concentrations indicates that the mineral crystals were undergoing dissolution with a preferential removal of B-type CO<sub>3</sub><sup>2-</sup> when initially exposed to the NaCl solutions (Figure 3B-C). This was supported by the decrease in the c-axis spacing, particularly seen in the 3% CO<sub>3</sub><sup>2-</sup> apatite exposed to NaCl at pH 7.4 as compared to the unexposed crystals (Figure 4A) [29]. The increased labile CO<sub>3</sub><sup>2</sup> suggests that the CO<sub>3</sub><sup>2</sup> in solution may be integrated through ionic exchange in the hydrated layer once recrystallization occurs [27]. In addition, the general decrease of Na<sup>+</sup> content in the solution (Figure 6C) suggests that the initial 3 wt% CO<sub>3</sub><sup>2-</sup> is likely taking up Na<sup>+</sup> from the solution in conjunction with the change in CO<sub>3</sub><sup>2-</sup> content during recrystallization. Conversely, the 7% CO<sub>3</sub><sup>2-</sup> apatite exhibited fewer modifications of the CO<sub>3</sub><sup>2-</sup> content with exposure than the 3% CO<sub>3</sub><sup>2</sup>- apatite (Figure 2). In these apatites, the lack of change in labile and B-type with only general decreases in A-type CO<sub>3</sub><sup>2-</sup> content suggests that the higher carbonated mineral preferentially releases the CO<sub>3</sub><sup>2-</sup> in the apatite channels when exposed to NaCl (Figure 3B-C) [36]. This agrees with previous studies indicating a relationship between A-type CO<sub>3</sub><sup>2-</sup> and Na<sup>+</sup> for highly carbonated apatites synthesized at higher temperatures as created in this study [15]. Due to the small amount of A-type dissolved, the lattice spacing was not affected (Figure 3A). Regardless of the location of the carbonate loss, the increased crystallite size for crystals exposed to NaCl compared to the unexposed crystals (Figure 5A-B) may be explained by the CO<sub>3</sub><sup>2</sup>removal from the lattice as this may lead to the formation of less distorted crystals, which reduces the crystal energy and promotes crystal growth [29,50,51]. Overall, exposure of apatite to NaCl solutions resulted in larger apatite crystals with modified CO<sub>3</sub><sup>2-</sup> distributions that are dependent on the initial apatite composition itself, rather than pH or NaCl concentration.

Apatite crystals in NaCl exhibited the expected behaviors of a conventional dissolution/recrystallization and release of buffering ions; however, this was not the case for KCl. Much like in NaCl, the presence of mineral in KCl increased the solution pH, indicating that buffering ions may be released (Figure 1A). The  $\Delta pH$  also increased with reduced pH<sub>i</sub> and reduced KCl concentration as seen with NaCl. However, the similarities end there. The significantly less mass lost in apatite in KCl compared to its NaCl counterpart (Figure 1B) suggests that the increase in solution pH is not caused by mineral dissolution. Instead, K<sup>+</sup> may

have protective effects against dissolution of apatite itself [52,53]. Furthermore, the 3% CO<sub>3</sub><sup>2</sup>apatite did not exhibit the expected loss of CO<sub>3</sub><sup>2</sup> with exposure like NaCl (Figure 1B and Figure 2). Instead, the CO<sub>3</sub><sup>2</sup> levels in apatite increased with KCl exposure, further supporting the expected decrease in crystallite size with increasing CO<sub>3</sub><sup>2-</sup> (Figure 5A-B). Without apatite dissolution or the release of CO<sub>3</sub><sup>2-</sup> buffering ions, the measured increase in pH may be caused by the sequestration of protons (H<sup>+</sup>) in the metastable hydrated surface layer and/or the protonated states of PO<sub>4</sub><sup>3-</sup> or CO<sub>3</sub><sup>2-</sup> to create HPO<sub>4</sub><sup>2-</sup> and HCO<sub>3</sub><sup>-</sup> substitution in the apatite lattice or within the hydrated layer [36,54–56]. To elaborate, the final pH for all conditions was ~pH 7, resulting in the ionization of the solution PO<sub>4</sub><sup>3-</sup> into HPO<sub>4</sub><sup>2-</sup>. HPO<sub>4</sub><sup>2-</sup> is known to integrate within the Btype sites to replace  $CO_3^{2-}$  in the lattice as well as within the amorphous apatite surface layer [27,55,57]. This may provide a possible explanation for the dissolution-free buffering. Accumulation of positively charged H<sup>+</sup> into the hydrated layer could also recruit negatively charged CO<sub>3</sub><sup>2</sup>, which may explain both the buffering and the increased CO<sub>3</sub><sup>2</sup> content. Overall, this data suggests that having K<sup>+</sup> in the solution may be protective against dissolution of apatites compared to the dissolving nature of Na<sup>+</sup> solutions as seen in this study. To our knowledge, this is the first time that this behavior has been described.

With so many possible ion exchanges, it was necessary to determine how KCl exposure affected the location of the CO<sub>3</sub><sup>2</sup>. Once again, exposure to KCl had significantly different effects on CO<sub>3</sub><sup>2-</sup> location than NaCl. The 3% CO<sub>3</sub><sup>2-</sup> apatites in KCl showed a general decrease in A-type CO<sub>3</sub><sup>2</sup>- and an increase in B-type CO<sub>3</sub><sup>2</sup>- compared to the unexposed mineral (Figure 3A). It previously has been shown that the presence of K<sup>+</sup> during crystal formation shifts the location of CO<sub>3</sub><sup>2</sup> away from the B-type location and into the A-type locations [22], the opposite of what was seen here. This data indicates that the K<sup>+</sup> in the KCl is likely not integrating into the lattice of the exposed apatites, but it may be serving as a protective barrier in the solution instead, perhaps in a Stern-like layer [58,59] or in the hydrated layer. The K<sup>+</sup> levels in the solution showed mixed results supporting the idea that there is no significant exchange of K<sup>+</sup> between the solution and the mineral lattice (Figure 6D). Interestingly, the increase in B-type CO<sub>3</sub><sup>2-</sup> did not significantly affect the lattice spacing of the crystals (Figure 4A). This could be due to the smaller number of CO<sub>3</sub><sup>2</sup>- exchanges in the KCl sample as compared to the NaCl samples. In addition, the lack of change of labile CO<sub>3</sub><sup>2-</sup> in the hydrated layer for the 3% CO<sub>3</sub><sup>2-</sup> apatites in KCl (Figure 3C) may point to an increased uptake of H<sup>+</sup> in the hydrated layer. Because HPO<sub>4</sub><sup>2-</sup> substitutes for the PO<sub>4</sub><sup>3-</sup> groups/B-type sites within apatite, this may be through protonation of  $HCO_3^-$  or  $HPO_4^{2-}$  as a better mechanism for reducing H<sup>+</sup> in the solution than HPO<sub>4</sub><sup>2-</sup> substitution within the lattice. At an initial 7% CO<sub>3</sub><sup>2</sup>, the apatites exhibited no change in A, B, or labile-type apatite with exposure, further supporting the idea that K<sup>+</sup> acts as a protectant to the mineral crystals, compared to Na.

In terms of the independent variables of pH and concentration, there were surprisingly few correlations with mineral properties. The concentration of both NaCl and KCl as well as the pH<sub>i</sub> significantly affected the  $\Delta$ pH of the solution (Figure 1A). In addition, the pH<sub>i</sub> may have had slight effects on the CO<sub>3</sub><sup>2-</sup> content and location. However, these were rarely the primary factors responsible for the measured changes in mineral properties. It is possible that the time frame of 3 days and the rapid increase from pH 5.5 to ~pH 7-8, especially for KCl, may explain the lack of effect of pH<sub>i</sub> as the mineral in all conditions generally equilibrated within the first hour

(Supplemental Figure 2-3). Previously, the initial pH exhibited more significant effects in solutions with high buffering capacities unlike the ones used here [60]. Instead, these apatites behaved more like apatite dissolution in water [44]. In terms of concentration, it has previously been shown that the effect of concentration on the dissolution properties of apatite is dependent on the type of simple salt [61], where NaCl may have relatively little effect on the dissolution mechanism supporting the data collected here.

#### 4.1. Limitations

Biological and biomimetic carbonated apatites have a substantial amount of HPO<sub>4</sub><sup>2-</sup> in the hydrated surface layer and within the crystalline apatite core [24]. Due to the increased pH, low mass loss, and increased CO<sub>3</sub><sup>2-</sup> content after exposure, HPO<sub>4</sub><sup>2-</sup> may contribute to ionic substitution and dissolution in this study. Therefore, future studies determining the role of HPO<sub>4</sub><sup>2-</sup> in Na<sup>+</sup>- and K<sup>+</sup>-rich solutions will be important to understand the mechanism.

In addition, the solutions used here did not include other ions such as phosphate. Phosphate is a necessary component of saliva as well as other solutions used in medical research laboratories to prevent dissolution and alteration of mineral and calcified tissues [49,62,63]. Thus, future studies identifying this mechanism will be needed to fully understand carbonated apatite mineral dissolution in Na- and K-rich solutions with physiological phosphate conditions.

Furthermore, the conditions shown here were performed in triplicate. While the standard deviations were relatively small for most of the dependent factors, more replicates would be needed in future studies to further determine the statistical power.

# 5. Conclusions

The effect of variations in solution pH and cationic content on biomimetic tooth mineral structure and composition was investigated. It was found that, Na<sup>+</sup> causes dissolution of the mineral, resulting in greater release of CO<sub>3</sub><sup>2-</sup> (primarily B-type CO<sub>3</sub><sup>2-</sup> at low initial wt% CO<sub>3</sub><sup>2-</sup> and primarily A-type CO<sub>3</sub><sup>2-</sup> at high starting CO<sub>3</sub><sup>2-</sup> wt%), which increases the crystallite length and width as well as decreases the overall mass. This suggests that the apatite mineral undergoes classical dissolution and recrystallization in Na-rich solutions. On the other hand, KCl appears to protect the mineral from dissolution, resulting in less mass loss after exposure and retention of A-type, B-type, and labile CO<sub>3</sub><sup>2-</sup> as well as the crystalline lattice. Despite this lack of dissolution, the apatite was still able to buffer the acidic solutions likely because of H<sup>+</sup> sequestration. Revealing the phenomena between Na<sup>+</sup>, K<sup>+</sup>, and biomimetic apatites could aid in the development of treatments for the prevention of tooth dissolution. It also may provide some insight as to why K-rich diets aid in bone health while Na-rich diets are detrimental to bone.

# 6. Acknowledgements

We would like to acknowledge the Center for Environmental Science and Engineering (CESE) and the Institute of Materials Science (IMS) at the University of Connecticut for their assistance. Funding was provided by the University of Connecticut's Summer Dental Research Program for Katherine Peccerillo as well as the NSF CAREER grant [grant number 2044870] for Alix Deymier.

## 7. References

- [1] G. Singh, E. Iyer, H. Malik, Relative Changes in Salivary Sodium and Potassium in Relation to Exposure to High G Stress, Med J Armed Forces India 50 (1994) 261–265. https://doi.org/10.1016/S0377-1237(17)31082-1.
- [2] N.A. Thorn, I.L. Schwartz, J.H. Thaysen, Effect of Sodium Restriction on Secretion of Sodium and Potassium in Human Parotid Saliva, Journal of Applied Physiology 9 (1956) 477–480. https://doi.org/10.1152/jappl.1956.9.3.477.
- [3] C. Simões, I. Caeiro, L. Carreira, F.C. e Silva, E. Lamy, How Different Snacks Produce a Distinct Effect in Salivary Protein Composition, Molecules 26 (2021) 2403. https://doi.org/10.3390/molecules26092403.
- [4] A. Almståhl, M. Wikström, Electrolytes in stimulated whole saliva in individuals with hyposalivation of different origins, Archives of Oral Biology 48 (2003) 337–344. https://doi.org/10.1016/S0003-9969(02)00200-5.
- [5] C. Labat, S. Thul, J. Pirault, M. Temmar, S.N. Thornton, A. Benetos, M. Bäck, Differential associations for salivary sodium, potassium, calcium, and phosphate levels with carotid intima media thickness, heart rate, and arterial stiffness, Disease Markers 2018 (2018). https://doi.org/10.1155/2018/3152146.
- [6] B. Kallapur, K. Ramalingam, Bastian, A. Mujib, A. Sarkar, S. Sethuraman, Quantitative estimation of sodium, potassium and total protein in saliva of diabetic smokers and nonsmokers: A novel study, J Nat Sci Biol Med 4 (2013) 341–345. https://doi.org/10.4103/0976-9668.117006.
- [7] T. Dhondup, Q. Qian, Acid-Base and Electrolyte Disorders in Patients with and without Chronic Kidney Disease: An Update, Kidney Diseases 3 (2017) 136–148. https://doi.org/10.1159/000479968.
- [8] E.A.A. Neel, A. Aljabo, A. Strange, S. Ibrahim, M. Coathup, A.M. Young, L. Bozec, V. Mudera, Demineralization–remineralization dynamics in teeth and bone, International Journal of Nanomedicine 11 (2016) 4743–4763. https://doi.org/10.2147/IJN.S107624.
- [9] A.B. Sønju Clasen, I.E. Ruyter, Quantitative determination of type A and type B carbonate in human deciduous and permanent enamel by means of Fourier transform infrared spectrometry., Advances in Dental Research 11 (1997) 523–527. https://doi.org/10.1177/08959374970110042101.
- [10] J. De Dios Teruel, A. Alcolea, A. Hernández, A.J.O. Ruiz, Comparison of chemical composition of enamel and dentine in human, bovine, porcine and ovine teeth, Archives of Oral Biology 60 (2015) 768–775. https://doi.org/10.1016/j.archoralbio.2015.01.014.
- [11] A. Bigi, E. Boanini, M. Gazzano, Ion substitution in biological and synthetic apatites, in: Biomineralization and Biomaterials, Elsevier, 2016: pp. 235–266. https://doi.org/10.1016/B978-1-78242-338-6.00008-9.
- [12] R.D. Shannon, Revised effective ionic radii and systematic studies of interatomic distances in halides and chalcogenides, Acta Cryst A 32 (1976) 751–767. https://doi.org/10.1107/S0567739476001551.
- [13] S. Peroos, Z. Du, N.H. De Leeuw, A computer modelling study of the uptake, structure and distribution of carbonate defects in hydroxy-apatite, Biomaterials 27 (2006) 2150–2161. https://doi.org/10.1016/j.biomaterials.2005.09.025.
- [14] O.F. Yasar, W.-C. Liao, R. Mathew, Y. Yu, B. Stevensson, Y. Liu, Z. Shen, M. Edén, The Carbonate and Sodium Environments in Precipitated and Biomimetic Calcium Hydroxy-Carbonate Apatite Contrasted with Bone Mineral: Structural Insights from Solid-State NMR, The Journal of Physical Chemistry C 125 (2021) 10572–10592. https://doi.org/10.1021/ACS.JPCC.0C11389.

- [15] C.H. Yoder, M.M. Bollmeyer, K.R. Stepien, R.N. Dudrick, The effect of incorporated carbonate and sodium on the IR spectra of A- and AB-type carbonated apatites, American Mineralogist 104 (2019) 869–877. https://doi.org/10.2138/am-2019-6800.
- [16] E.A.P. De Maeyer, R.M.H. Verbeeck, Possible Substitution Mechanisms for Sodium and Carbonate in Calciumhydroxyapatite, Bulletin Des Sociétés Chimiques Belges 102 (1993) 601–609. https://doi.org/10.1002/bscb.19931020907.
- [17] F.C.M. Driessens, R.M.H. Verbeeck, H.J.M. Heijligers, Some physical properties of Na- and CO3-containing apatites synthesized at high temperatures, Inorganica Chimica Acta 80 (1983) 19–23. https://doi.org/10.1016/S0020-1693(00)91256-8.
- [18] S. Kannan, J.M.G. Ventura, J.M.F. Ferreira, Synthesis and thermal stability of potassium substituted hydroxyapatites and hydroxyapatite/β-tricalciumphosphate mixtures, Ceramics International 33 (2007) 1489–1494. https://doi.org/10.1016/j.ceramint.2006.05.016.
- [19] D.R. Simpson, Substitutions in apatite: I. Potassium-bearing apatite, The American Mineralogist 53 (1968) 432–444.
- [20] R.M.H. Verbeeck, E.A.P. De Maeyer, F.C.M. Driessens, Stoichiometry of Potassium- and Carbonate-Containing Apatites Synthesized by Solid State Reactions, Inorganic Chemistry 34 (1995) 2084–2088. https://doi.org/10.1021/ic00112a021.
- [21] D. A. Nowicki, J.M. S. Skakle, I. R. Gibson, Potassium—carbonate co-substituted hydroxyapatite compositions: maximising the level of carbonate uptake for potential CO 2 utilisation options, Materials Advances 3 (2022) 1713–1728. https://doi.org/10.1039/D1MA00676B.
- [22] S.L. Wong, C. Drouet, A. Deymier, Carbonate environment changes with Na or K substitution in biomimetic apatites, Materialia 29 (2023) 101795. https://doi.org/10.1016/j.mtla.2023.101795.
- [23] T. Kono, T. Sakae, H. Nakada, T. Kaneda, H. Okada, Confusion between Carbonate Apatite and Biological Apatite (Carbonated Hydroxyapatite) in Bone and Teeth, Minerals 12 (2022) 170. https://doi.org/10.3390/min12020170.
- [24] C. Combes, S. Cazalbou, C. Rey, Apatite biominerals, Minerals 6 (2016) 34. https://doi.org/10.3390/min6020034.
- [25] M.E. Fleet, X. Liu, Carbonate in Synthetic and Biological Apatites, n.d.
- [26] Y. Pan, M.E. Fleet, Compositions of the Apatite-Group Minerals: Substitution Mechanisms and Controlling Factors, Reviews in Mineralogy and Geochemistry 48 (2002) 13–49. https://doi.org/10.2138/rmg.2002.48.2.
- [27] D. Eichert, C. Combes, C. Drouet, C. Rey, Formation and Evolution of Hydrated Surface Layers of Apatites, Key Engineering Materials 284–286 (2005) 3–6. https://doi.org/10.4028/www.scientific.net/kem.284-286.3.
- [28] H. Madupalli, B. Pavan, M.M.J. Tecklenburg, Carbonate substitution in the mineral component of bone: Discriminating the structural changes, simultaneously imposed by carbonate in A and B sites of apatite, Journal of Solid State Chemistry 255 (2017) 27–35. https://doi.org/10.1016/j.jssc.2017.07.025.
- [29] A.C. Deymier, A.K. Nair, B. Depalle, Z. Qin, K. Arcot, C. Drouet, C.H. Yoder, M.J. Buehler, S. Thomopoulos, G.M. Genin, J.D. Pasteris, Protein-free formation of bone-like apatite: New insights into the key role of carbonation, Biomaterials 127 (2017) 75–88. https://doi.org/10.1016/j.biomaterials.2017.02.029.
- [30] R.Z. Legeros, O.R. Trautz, J.P. Legeros, E. Klein, W.P. Shirra, Apatite Crystallites: Effects of Carbonate on Morphology, Science 155 (1967) 1409–1411. https://doi.org/10.1126/science.155.3768.1409.
- [31] A.A. Baig, J.L. Fox, J. Hsu, Z. Wang, M. Otsuka, W.I. Higuchi, R.Z. LeGeros, Effect of Carbonate Content and Crystallinity on the Metastable Equilibrium Solubility Behavior of Carbonated Apatites, Journal of Colloid and Interface Science 179 (1996) 608–617. https://doi.org/10.1006/jcis.1996.0255.

- [32] A.A. Baig, J.L. Fox, R.A. Young, Z. Wang, J. Hsu, W.I. Higuchi, A. Chhettry, H. Zhuang, M. Otsuka, Relationships among carbonated apatite solubility, crystallite size, and microstrain parameters, Calcified Tissue International 64 (1999) 437–449. https://doi.org/10.1007/PL00005826.
- [33] B. Wingender, M. Azuma, C. Krywka, P. Zaslansky, J. Boyle, A.C. Deymier, Carbonate substitution significantly affects the structure and mechanics of carbonated apatites, Acta Biomaterialia (2020).
- [34] G.H. Nancollas, B. Tomazic, Growth of calcium phosphate on hydroxyapatite crystals. Effect of supersaturation and ionic medium, Journal of Physical Chemistry 78 (1974) 2218–2225. https://doi.org/10.1021/j100615a007.
- [35] C.J.S. Ibsen, H. Leemreize, B.F. Mikladal, J. Skovgaard, M. Bremholm, J.R. Eltzholtz, B.B. Iversen, H. Birkedal, Alkali Counterions Impact Crystallization Kinetics of Apatite Nanocrystals from Amorphous Calcium Phosphate in Water at High pH, Crystal Growth and Design 18 (2018) 6723–6728. https://doi.org/10.1021/acs.cgd.8b01008.
- [36] M.E. Fleet, Infrared spectra of carbonate apatites: Evidence for a connection between bone mineral and body fluids, American Mineralogist 102 (2017) 149–157. https://doi.org/10.2138/am-2017-5704
- [37] M.S. Sader, K. Lewis, G.A. Soares, R.Z. Legeros, Simultaneous Incorporation of Magnesium and Carbonate in Apatite: Effect on Physico-chemical Properties, (2013). https://doi.org/10.1590/S1516-14392013005000046.
- [38] R.Z. LeGeros, T. Sakae, C. Bautista, M. Retino, J.P. LeGeros, Magnesium and carbonate in enamel and synthetic apatites., Advances in Dental Research 10 (1996) 225–231. https://doi.org/10.1177/08959374960100021801.
- [39] A. Joseph Nathanael, D. Mangalaraj, S.I. Hong, Y. Masuda, Y.H. Rhee, H.W. Kim, A.J. Nathanael, D. Mangalaraj, S.I. Hong, Y. Masuda, Y.H. Rhee, H.W. Kim, Influence of fluorine substitution on the morphology and structure of hydroxyapatite nanocrystals prepared by hydrothermal method, Materials Chemistry and Physics 137 (2013) 967–976. https://doi.org/10.1016/j.matchemphys.2012.11.010.
- [40] M. Crisostomo, C. Ureta, Salivary pH and Taste Sensitivity among Geriatric and Non-Geriatric Patients in a Tertiary Hospital: A Cross Sectional Study, Philippine Journal of Otolaryngology Head and Neck Surgery 34 (2019) 11–15. https://doi.org/10.32412/pjohns.v34i2.125.
- [41] M.J. Larsen, A.F. Jensen, D.M. Madsen, E.I.F. Pearce, Individual variations of pH, buffer capacity, and concentrations of calcium and phosphate in unstimulated whole saliva, Archives of Oral Biology 44 (1999) 111–117. https://doi.org/10.1016/S0003-9969(98)00108-3.
- [42] and M.C.H. van der M. Eve Donnelly, Adele L. Boskey, Shefford P. Baker, Effects of tissue age on bone tissue material composition and nanomechanical properties in the rat cortex, Journal of Biomedical Materials Research Part A 92 (2010) 1048–1056. https://doi.org/10.1161/CIRCULATIONAHA.110.956839.
- [43] P.G. Spizzirri, N.J. Cochrane, S. Prawer, E.C. Reynolds, A Comparative Study of Carbonate Determination in Human Teeth Using Raman Spectroscopy, Caries Research 46 (2012) 353–360. https://doi.org/10.1159/000337398.
- [44] M.M. Moynahan, S.L. Wong, A.C. Deymier, Beyond dissolution: Xerostomia rinses affect composition and structure of biomimetic dental mineral in vitro, PLoS ONE 16 (2021) 5–7. https://doi.org/10.1371/journal.pone.0250822.
- [45] S.M. Barinov, I.V. Fadeeva, D. Ferro, J.V. Rau, S.N. Cesaro, V.S. Komlev, A.S. Fomin, Stabilization of Carbonate Hydroxyapatite by Isomorphic Substitutions of Sodium for Calcium, Russ. J. Inorg. Chem. 53 (2008) 164–168. https://doi.org/10.1134/S0036023608020022.
- [46] Z. Zyman, M. Tkachenko, Sodium-carbonate co-substituted hydroxyapatite ceramics, PAC 7 (2013) 153–157. https://doi.org/10.2298/PAC1304153Z.

- [47] D.A. Bushinsky, N.S. Krieger, Effects of acid on bone, Kidney International 101 (2022) 1160–1170. https://doi.org/10.1016/j.kint.2022.02.032.
- [48] N.S. Krieger, K.K. Frick, D.A. Bushinsky, Mechanism of acid-induced bone resorption, Current Opinion in Nephrology and Hypertension 13 (2004) 423–436. https://doi.org/10.1097/01.mnh.0000133975.32559.6b.
- [49] S.L. Wong, A.C. Deymier, Phosphate and buffer capacity effects on biomimetic carbonate apatite, Ceramics International 49 (2023) 12415–12422. https://doi.org/10.1016/j.ceramint.2022.12.101.
- [50] J.F. Ferguson, P.L. McCarty, Effects of carbonate and magnesium on calcium phosphate precipitation, Environ. Sci. Technol. 5 (1971) 534–540. https://doi.org/10.1021/es60053a005.
- [51] X. Cao, W. Harris, Carbonate and Magnesium Interactive Effect on Calcium Phosphate Precipitation, Environ. Sci. Technol. 42 (2008) 436–442. https://doi.org/10.1021/es0716709.
- [52] J. Ha, S.-A. Kim, K. Lim, S. Shin, The association of potassium intake with bone mineral density and the prevalence of osteoporosis among older Korean adults, Nutr Res Pract 14 (2020) 55–61. https://doi.org/10.4162/nrp.2020.14.1.55.
- [53] J. Green, C.R. Kleeman, Role of bone in regulation of systemic acid-base balance, Kidney International 39 (1991) 9–26. https://doi.org/10.1038/ki.1991.2.
- [54] J. Lemann, D.A. Bushinsky, L.L. Hamm, Bone buffering of acid and base in humans, American Journal of Physiology Renal Physiology 285 (2003). https://doi.org/10.1152/ajprenal.00115.2003.
- [55] S. Von Euw, Y. Wang, G. Laurent, C. Drouet, F. Babonneau, N. Nassif, T. Azaïs, Bone mineral: new insights into its chemical composition, Scientific Reports 9 (2019) 1–11. https://doi.org/10.1038/s41598-019-44620-6.
- [56] C. Combes, C. Rey, S. Mounic, Identification and evaluation of HPO4 ions in biomimetic poorly crystalline apatite and bone mineral, Key Engineering Materials 192–195 (2001) 143–146.
- [57] C. Drouet, M. Aufray, S. Rollin-Martinet, N. Vandecandelaère, D. Grossin, F. Rossignol, E. Champion, A. Navrotsky, C. Rey, Nanocrystalline apatites: The fundamental role of water, American Mineralogist 103 (2018) 550–564. https://doi.org/10.2138/am-2018-6415.
- [58] M.A. Brown, G.V. Bossa, S. May, Emergence of a Stern Layer from the Incorporation of Hydration Interactions into the Gouy–Chapman Model of the Electrical Double Layer, Langmuir 31 (2015) 11477–11483. https://doi.org/10.1021/acs.langmuir.5b02389.
- [59] I. Siretanu, D. Ebeling, M.P. Andersson, S.L.S. Stipp, A. Philipse, M.C. Stuart, D. Van Den Ende, F. Mugele, Direct observation of ionic structure at solid-liquid interfaces: a deep look into the Stern Layer, Sci Rep 4 (2014) 4956. https://doi.org/10.1038/srep04956.
- [60] N.X. West, J.A. Hughes, M. Addy, The effect of pH on the erosion of dentine and enamel by dietary acids in vitro, Journal of Oral Rehabilitation 28 (2008) 860–864. https://doi.org/10.1111/j.1365-2842.2001.00778.x.
- [61] S. Shimabayashi, M. Matsumoto, Non-stoichiometric Dissolution of Hydroxyapatite in the Presence of Simple Salts, Nippon Kagaku Kaishi 1993 (1993) 1118–1122. https://doi.org/10.1246/nikkashi.1993.1118.
- [62] S. Habelitz, G.W. Marshall, M. Balooch, S.J. Marshall, Nanoindentation and storage of teeth, Journal of Biomechanics 35 (2002) 995–998. https://doi.org/10.1016/S0021-9290(02)00039-8.
- [63] S.E. Strawn, J.M. White, G.W. Marshall, L. Gee, H.E. Goodis, S.J. Marshall, Spectroscopic changes in human dentine exposed to various storage solutions short term, Journal of Dentistry 24 (1996) 417–423. https://doi.org/10.1016/0300-5712(95)00106-9.

**Figure 1. pH and mass change after 3 days of mineral-solution exposure. A)** The delta pH increased after exposure to apatite with either 3 or 7 wt%  $CO_3^{2-}$ , indicating increased solution pH with trends in concentrations (0, 0.05, 0.1, 0.2 M). **B)** The mass of apatite decreased after exposure to the solution, especially for apatites with an initial 3 wt%  $CO_3^{2-}$  in water, NaCl, and KCl as well as 7 wt%  $CO_3^{2-}$  apatites in water and NaCl. Significance is indicated as p>0.05.

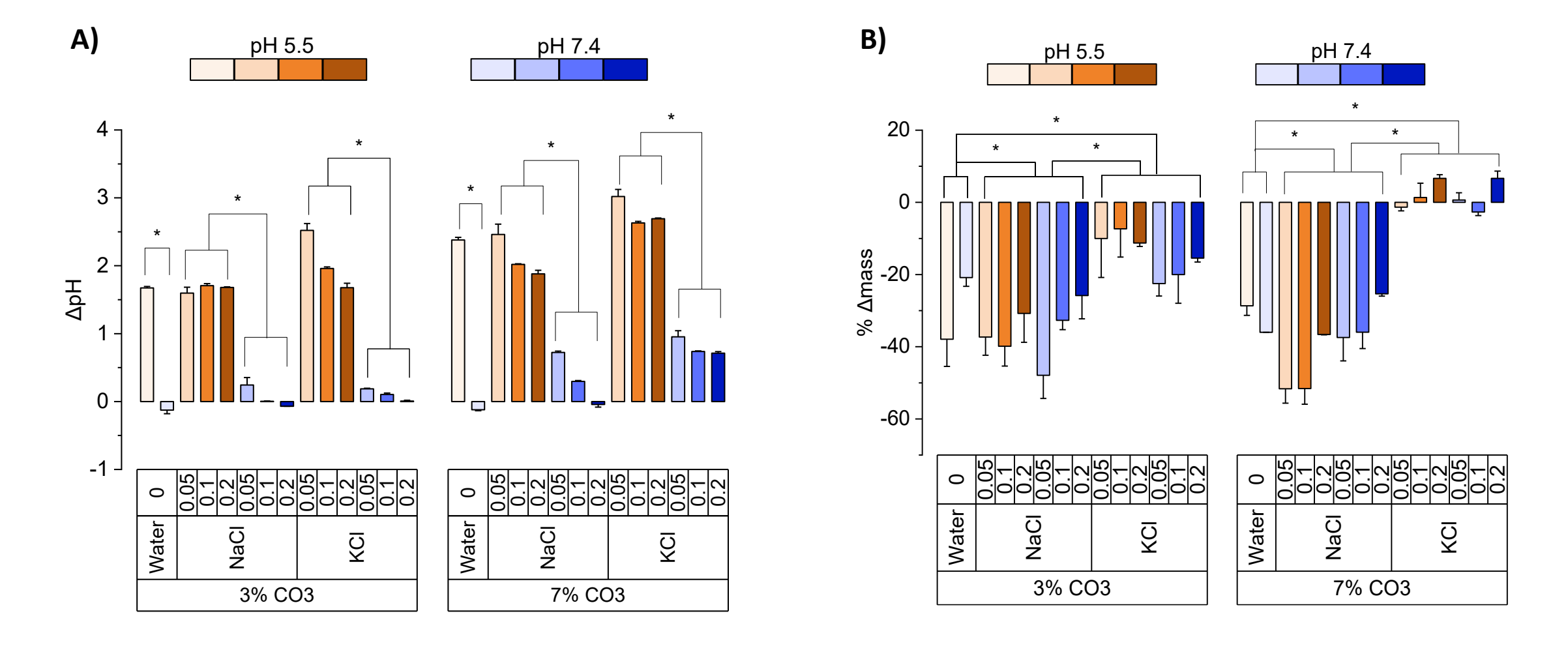


Figure 2. CO3/PO4 ratio of the apatite mineral. The overall increased % $\Delta$ CO3/PO4 in the initial 3 wt% CO<sub>3</sub><sup>2-</sup> apatites in KCl indicated more CO<sub>3</sub><sup>2-</sup> after exposure than water and NaCl. The means of NaCl/KCl, pH, and concentration groups were compared using 3-way ANOVA within each wt% CO<sub>3</sub><sup>2-</sup> group. Significance is p>0.05.

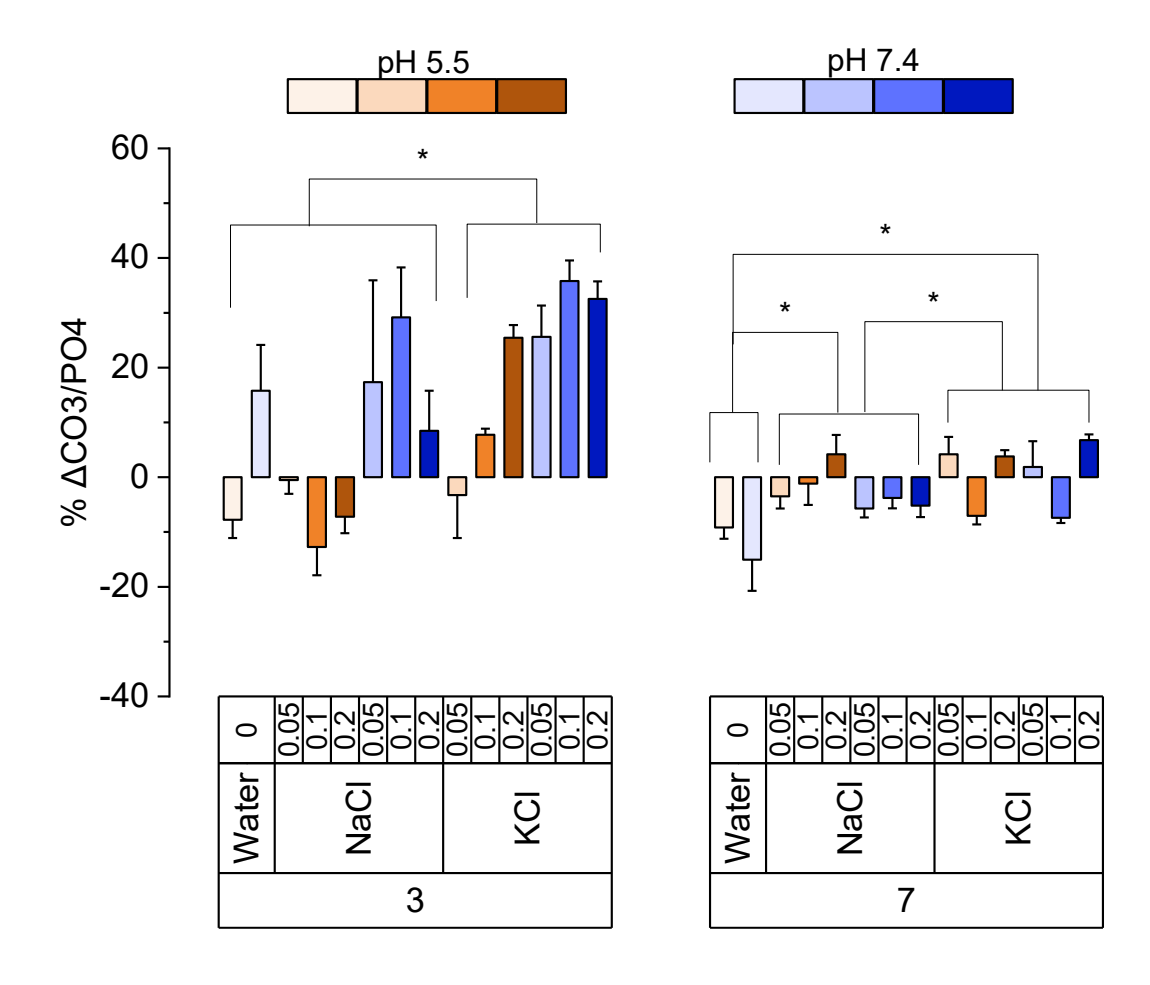


Figure 3. Relative amounts of the  $CO_3^{2-}$  types within the  $v_2$   $CO_3^{2-}$  region. A) A-type  $CO_3^{2-}$  generally did not change for apatites with an initial 3 wt%  $CO_3^{2-}$  after exposure to the NaCl or KCl compared to the unexposed apatite (Ctrl). Initial 7 wt%  $CO_3^{2-}$  in NaCl exhibited a trending decrease in A-type while KCl generally did not change. B) B-type  $CO_3^{2-}$  generally decreased for 3 wt%  $CO_3^{2-}$  apatites in NaCl but remained the same for KCl. C) Labile  $CO_3^{2-}$  had a trending increase for 3 wt%  $CO_3^{2-}$  apatites in NaCl only.

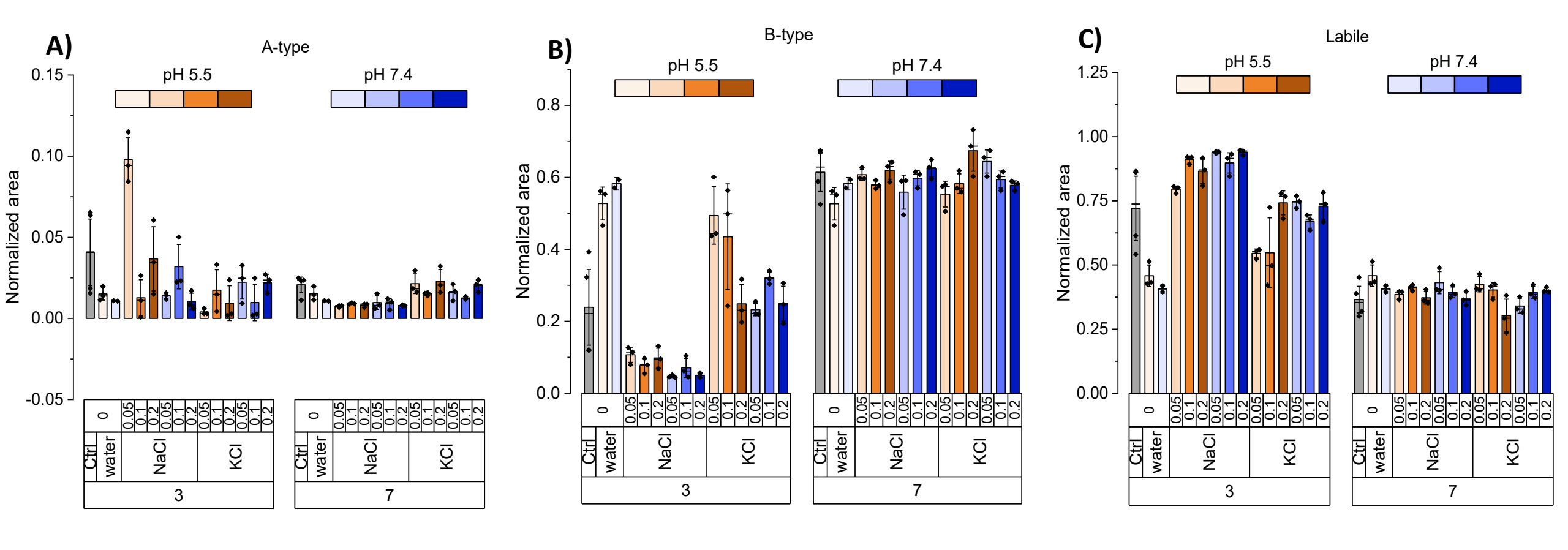


Figure 4. Apatite lattice spacing. The d-spacings of the A) c-axis (002) and B) a-axis (310) in all conditions, including the unexposed apatite mineral indicated as Ctrl.

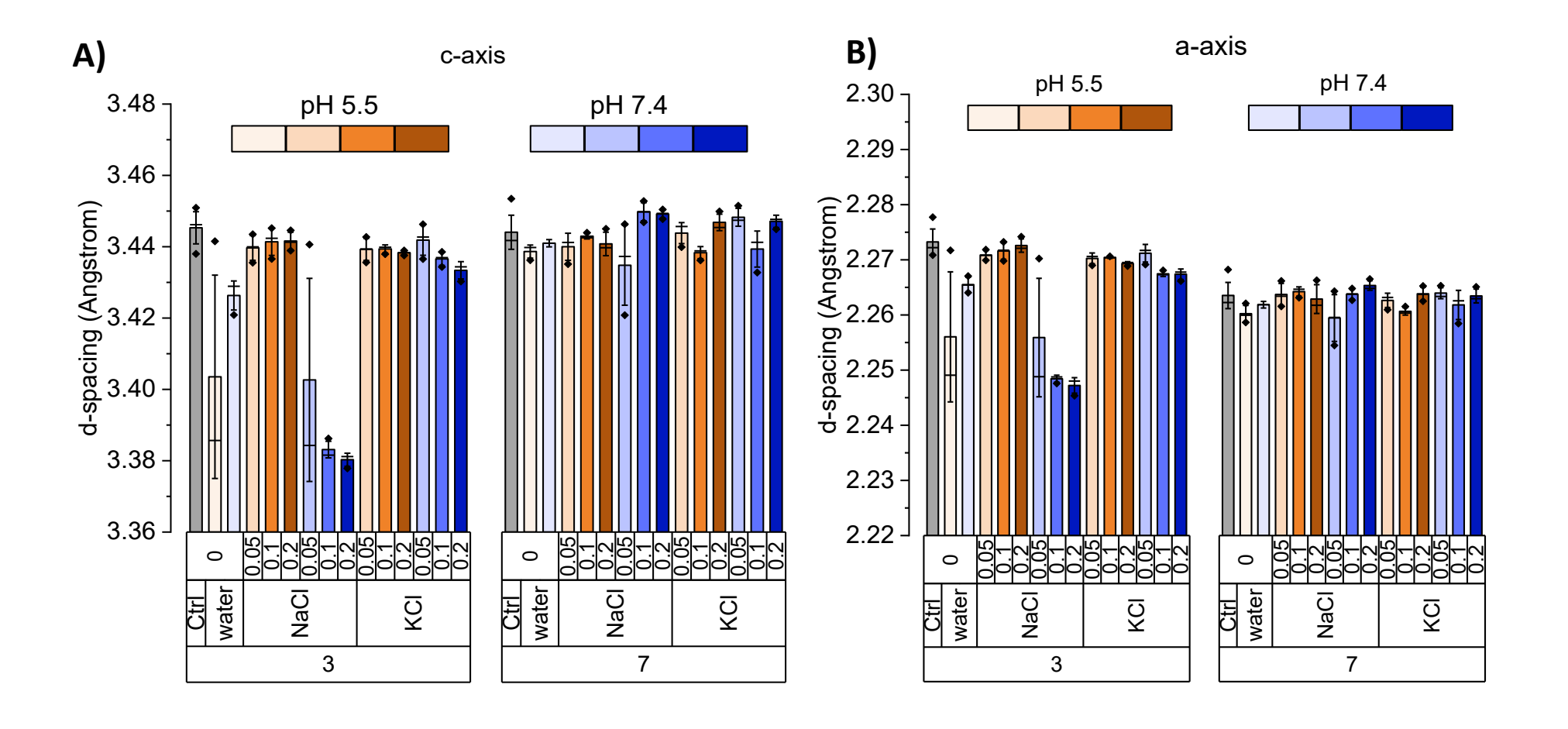
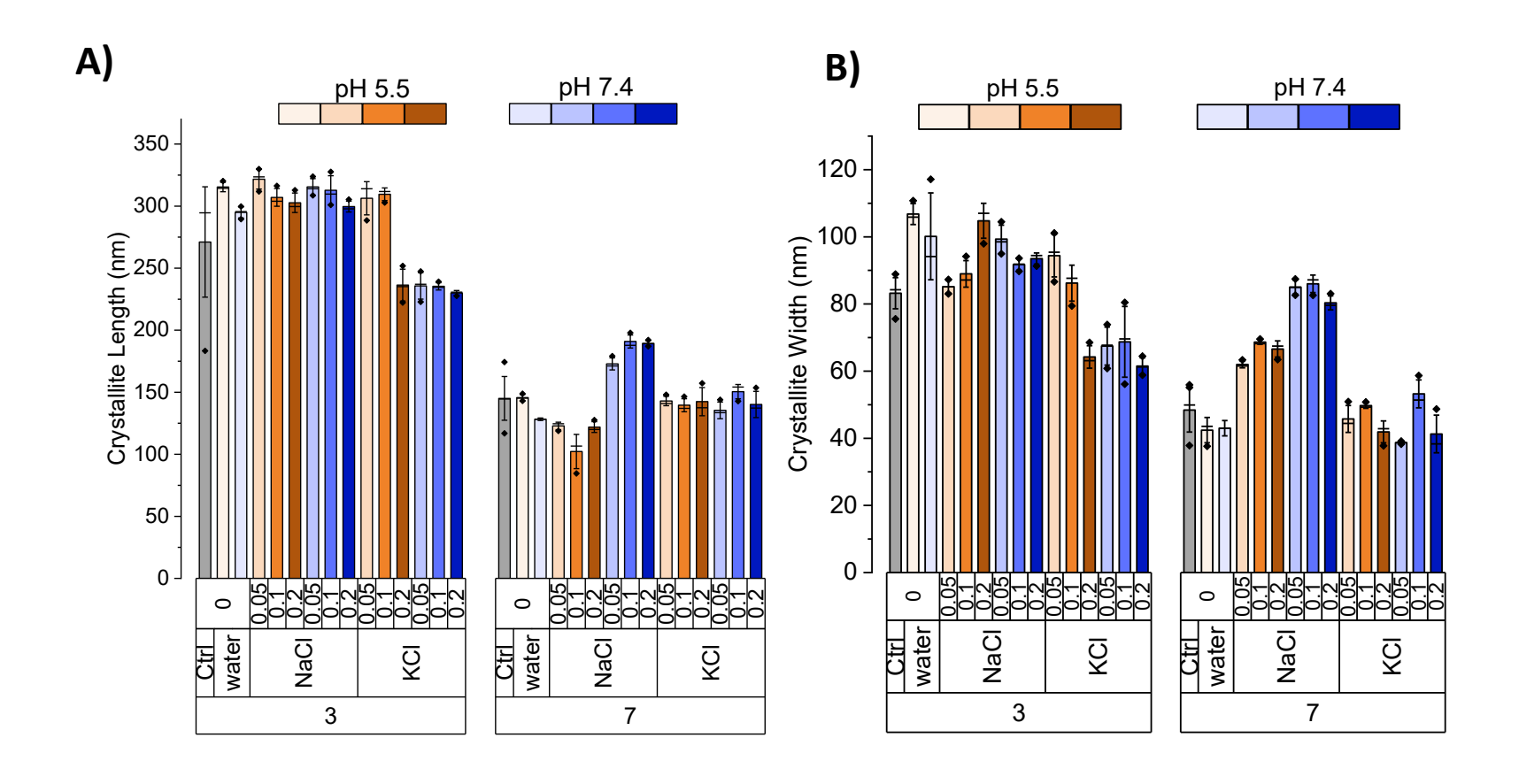


Figure 5. Crystallite sizes of apatite. The A) crystallite length and B) crystallite width using the (002) and (310) planes of apatite, respectively.



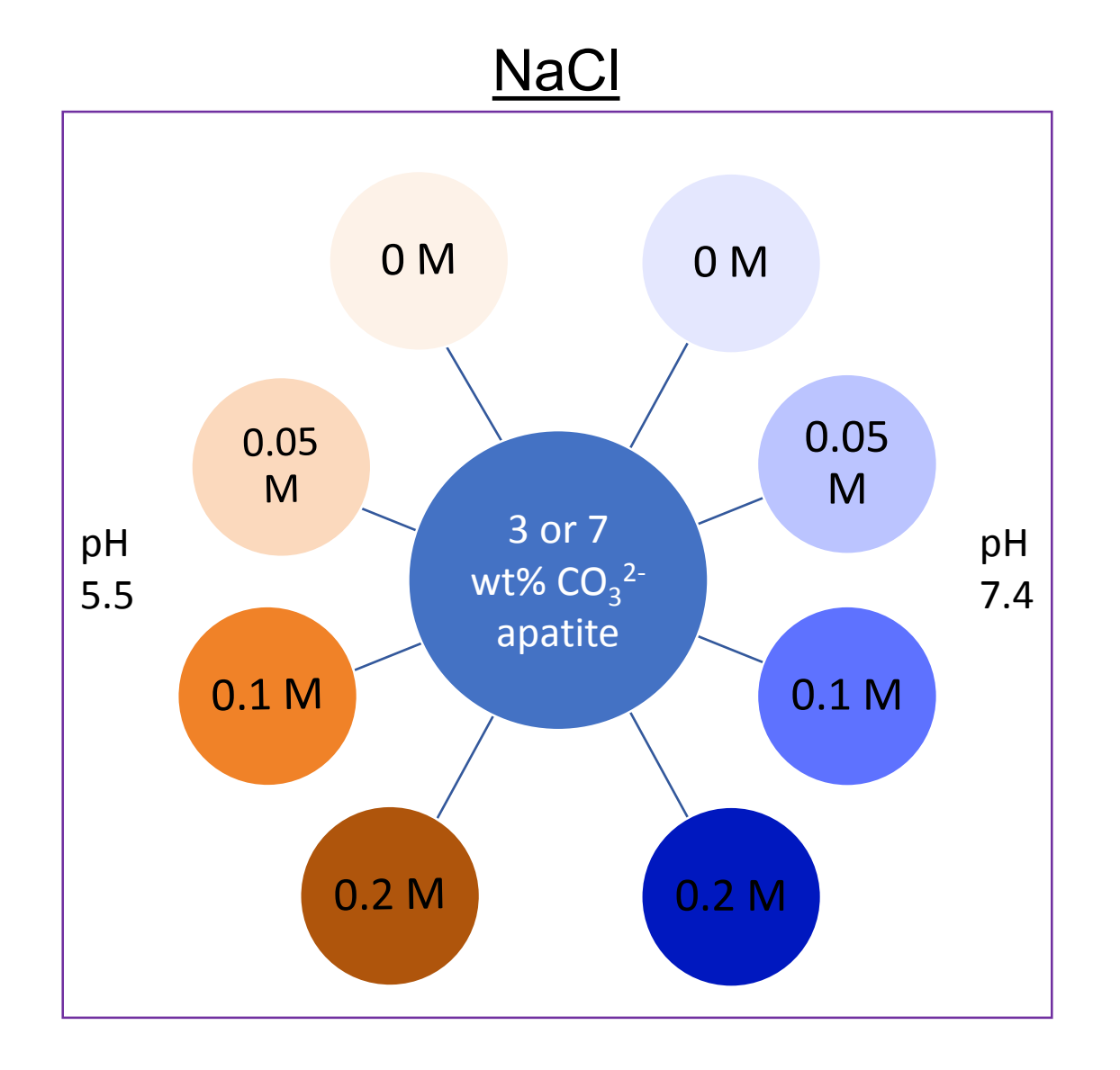
pH 5.5 pH 7.4 pH 5.5 pH 7.4 B) Figure 6. Solutes 120000 -60000 within the solution 105000 -50000 after exposure. A) 90000 -Calcium and B) 40000 75000 phosphorus 30000 60000 increased in the 20000 45000 solution after 10000 30000 exposure to the mineral. C) Sodium 15000 -0 generally decreased -10000 in the solution at Water Water NaC NaCl Water lower initial wt% Water Š  $\overline{\Omega}$ NaCl NaCl  $\overline{\Omega}$ <u>2</u>  $CO_3^{2-}$  while **D**) 3 7 3 potassium amounts fluctuated C) D) 750000 pH 5.5 pH 5.5 pH 7.4 pH 7.4 1000000 regardless of wt%, 800000 concentration, or 500000 pH. 600000 400000 250000 ΔK (ug/L) ΔNa (ug/L) 200000 -200000 -250000 -400000 -600000 -500000 -800000 -750000 -Water Water Water Water NaCl NaCl NaCl NaCl  $\overline{S}$  $\overline{\Omega}$  $\overline{\Omega}$ ठ

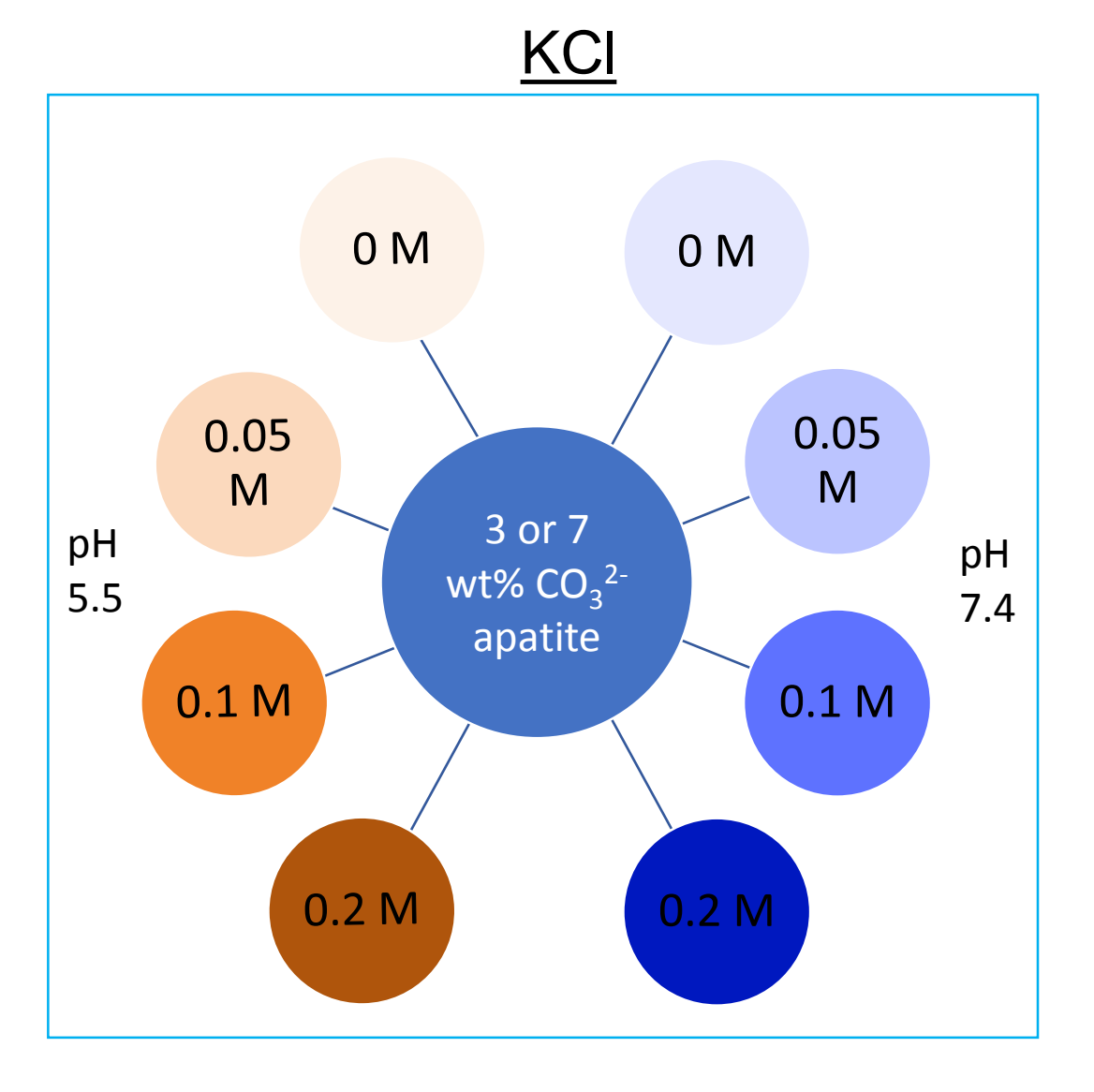
3

3

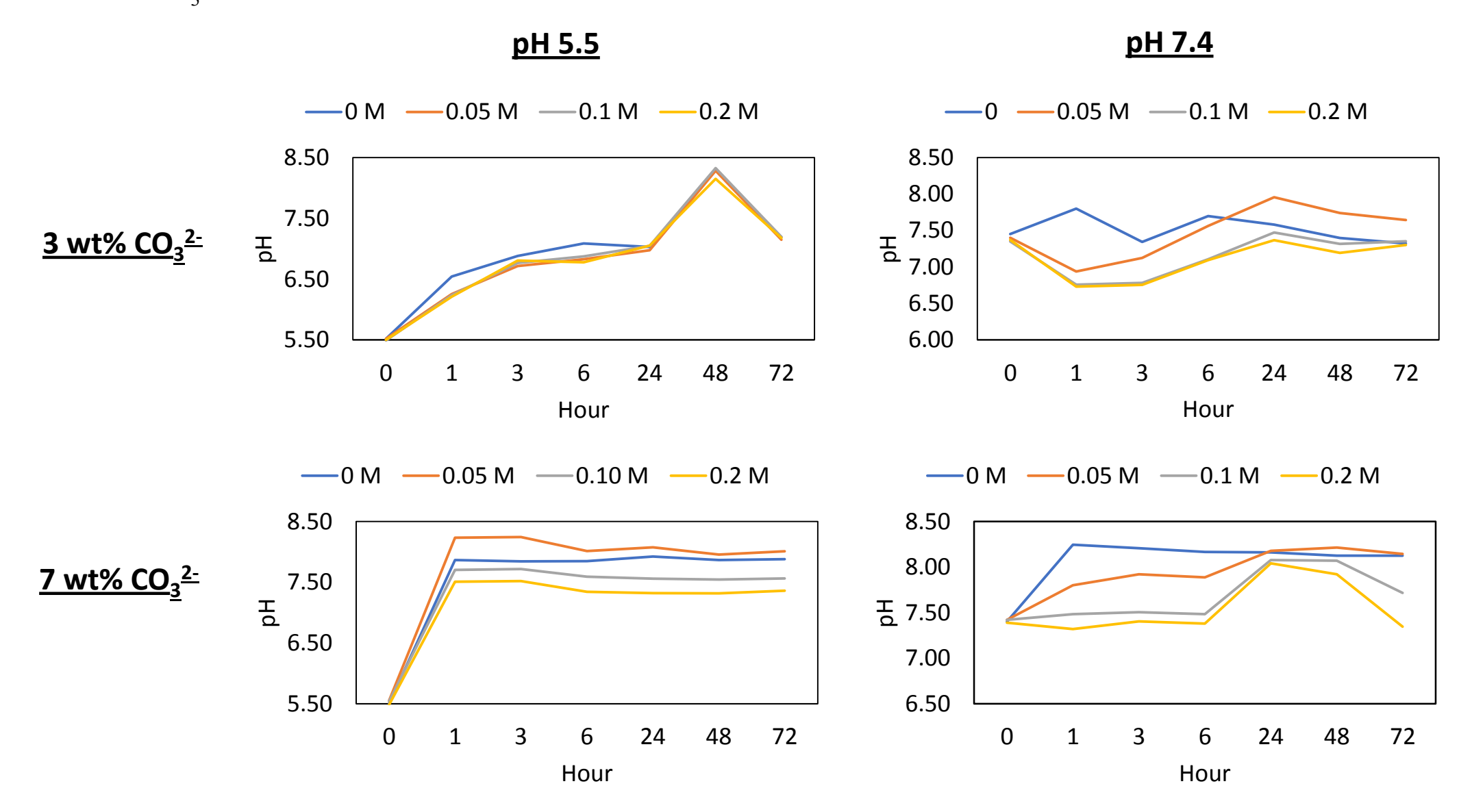
# Supplemental Figures

**Supplemental Figure 1. Schematic of experimental setup.** Biomimetic carbonated apatites with 3 or 7 wt% CO<sub>3</sub><sup>2-</sup> was exposed to either 0-0.2 M NaCl or KCl at pH 5.5 or 7.4 for 3 days.

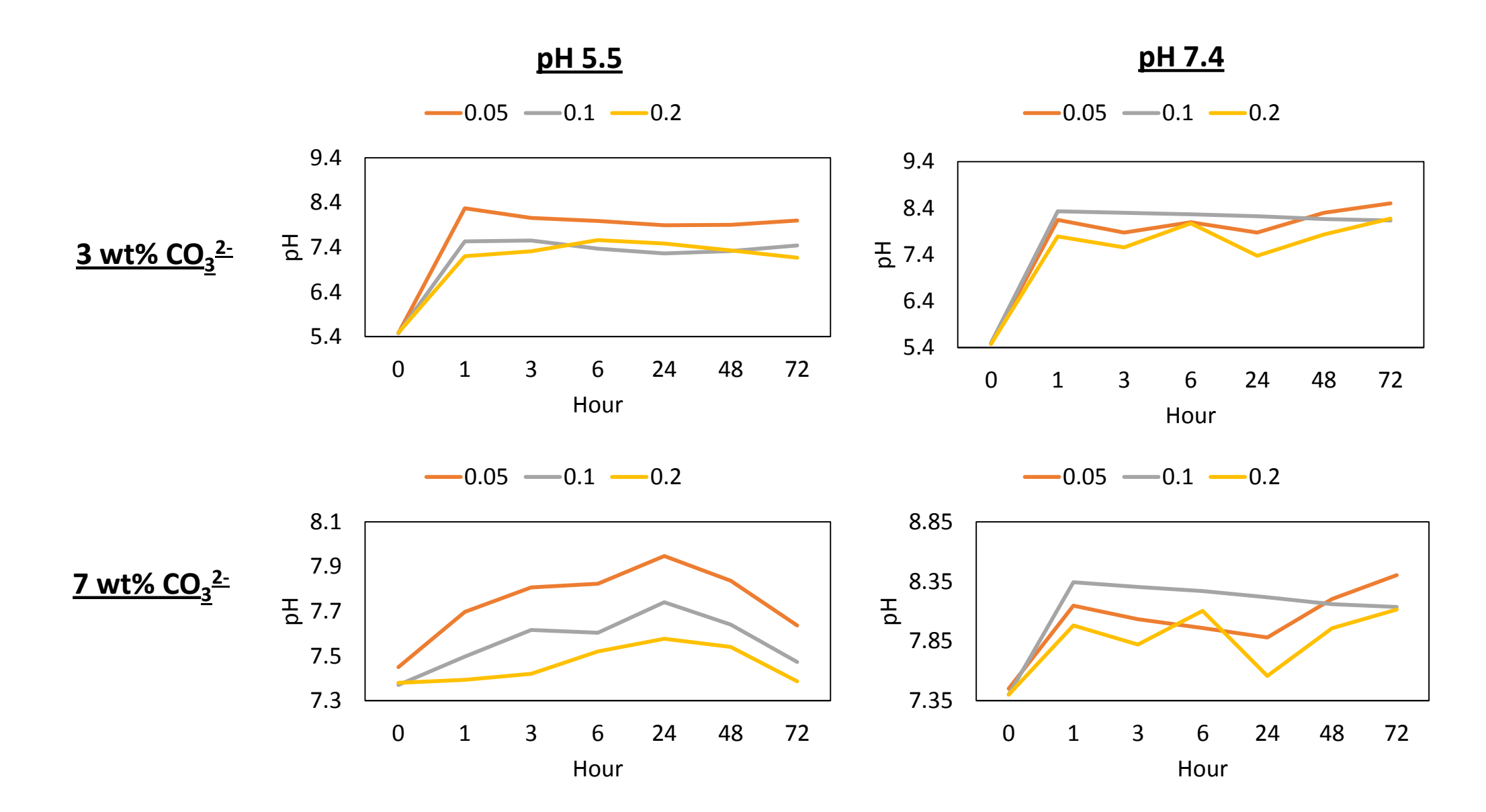




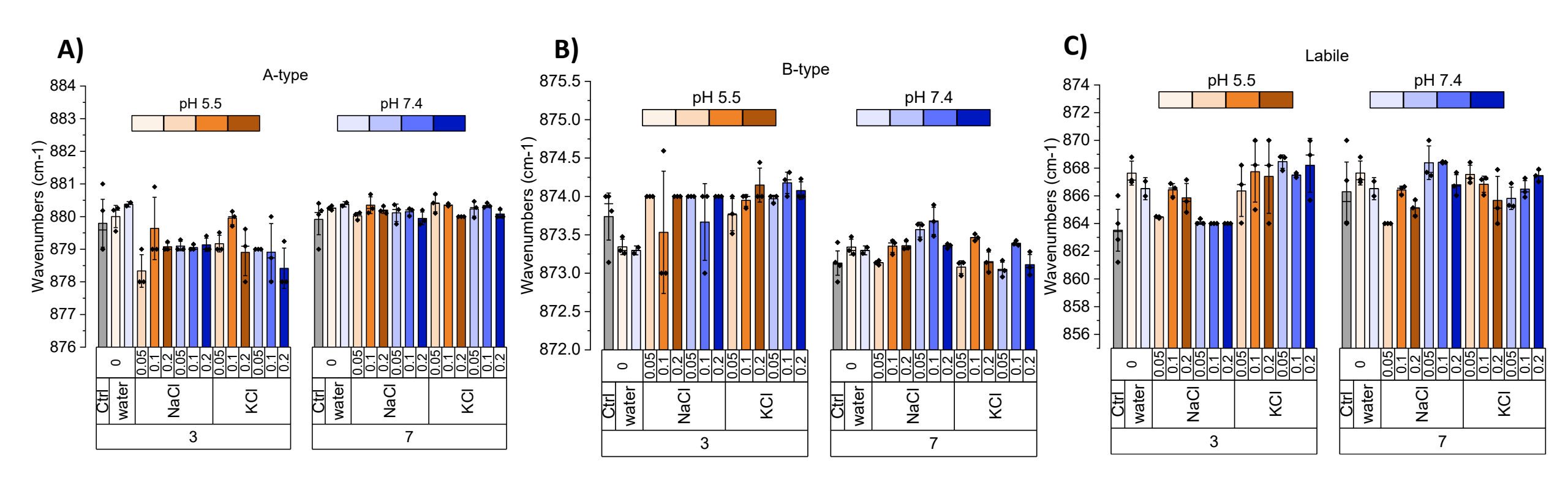
**Supplemental Figure 2.** pH over time for NaCl solution exposed to apatites with an initial (**A**, **B**) 3 wt%  $CO_3^{2-}$  or (**C**, **D**) 7 wt%  $CO_3^{2-}$ .



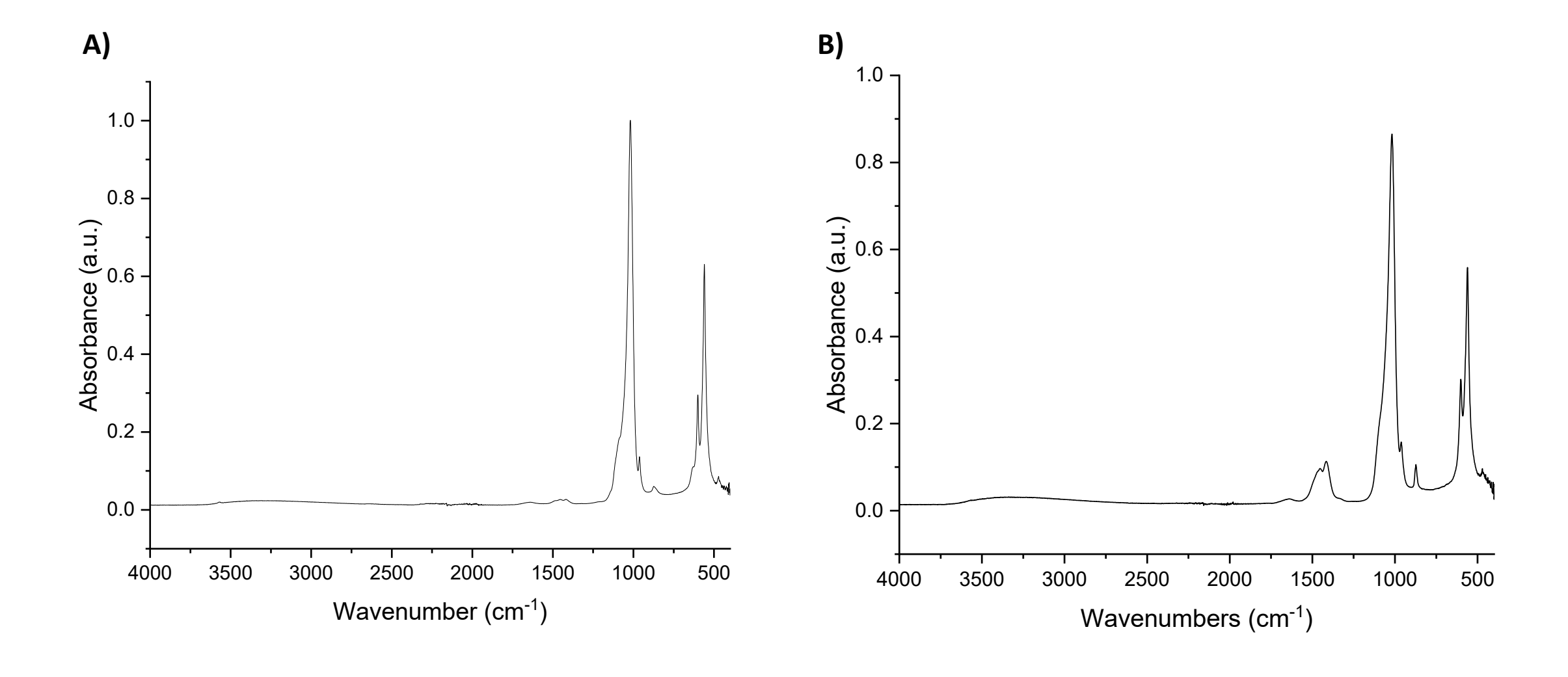
**Supplemental Figure 3.** pH over time for KCl solution exposed to apatites with an initial (**A**, **B**) 3 wt%  $CO_3^{2-}$  or (**C**, **D**) 7 wt%  $CO_3^{2-}$ .



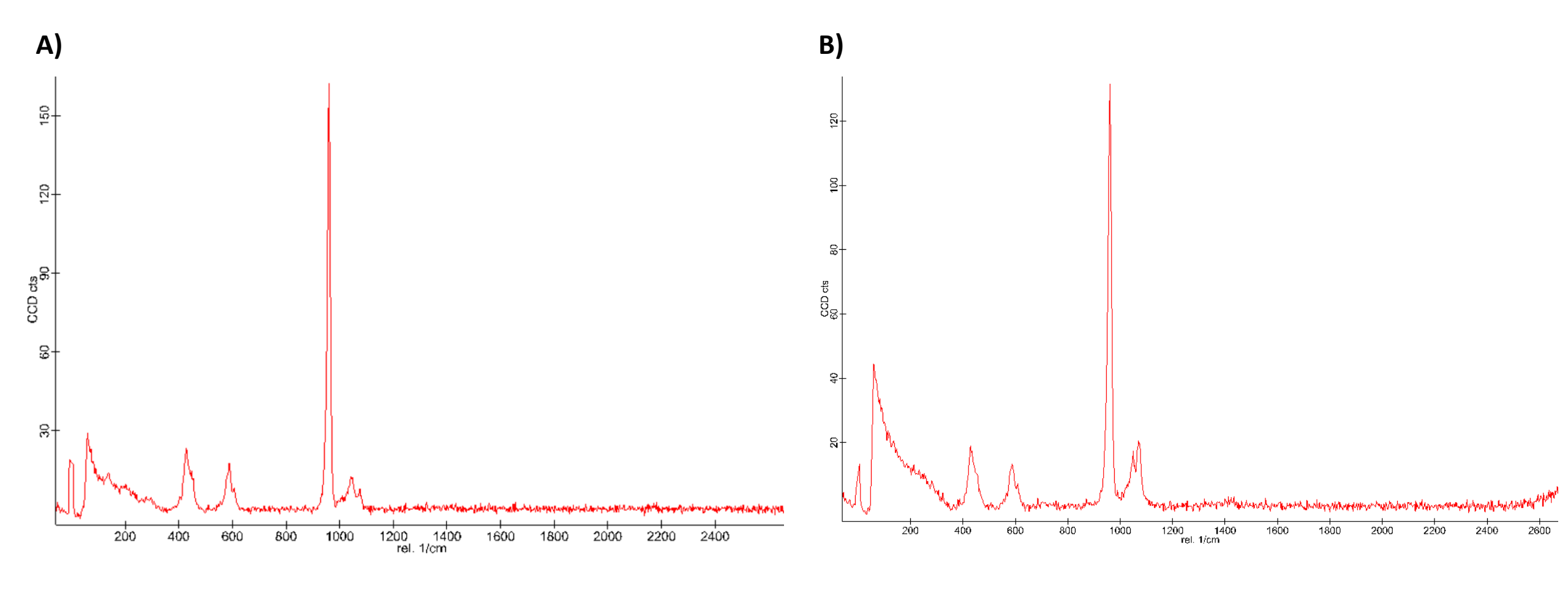
**Supplemental Figure 4.** FTIR waveumbers of **A)** A-type  $CO_3^{2-}$ , **B)** B-type  $CO_3^{2-}$ , **C)** labile  $CO_3^{2-}$  in the  $v_2 CO_3^{2-}$  region for all conditions.



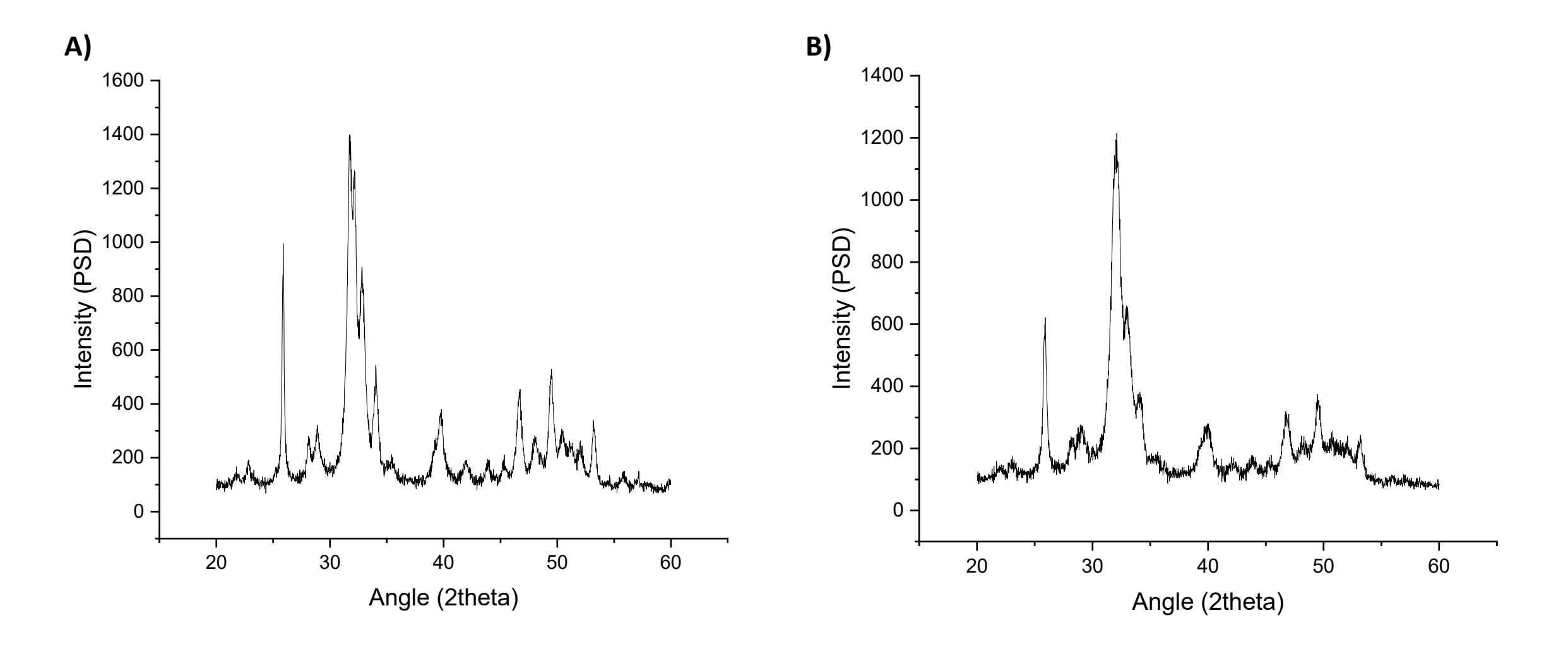
**Supplemental Figure 5.** A representative FTIR spectrum of biomimetic apatites with **(A)** 3 and **(B)** 7 wt% CO<sub>3</sub><sup>2-</sup> before exposure.



**Supplemental Figure 6.** A representative Raman spectrum of biomimetic apatites with **(A)** 3 and **(B)** 7 wt% CO<sub>3</sub><sup>2-</sup> before exposure to the KCl and NaCl solutions.



**Supplemental Figure 7.** A representative XRD pattern of biomimetic apatites with (a) 3 and (b) 7 wt% CO<sub>3</sub><sup>2-</sup> before exposure to the KCl and NaCl solutions.



**Supplemental Tables** 

Means that do not share a letter are significantly different.

## $\Delta pH$ stats

**Table 1.** The average  $\Delta pH$  of all conditions at pH 5.5 or pH 7.4 when considering the initial pH. Two 3-way ANOVAs were used to compare either 1) wt%  $CO_3^{2-}$ , NaCl vs KCl, and pH or 2) concentration, NaCl vs KCl, and pH.

Initial pH	Mean	Groups	Groups
5.5	2.13548	A	
7.4	0.26683		В

**Table 2.** The average  $\Delta pH$  when considering concentration.

3-way ANOVA comparisons: 1) concentration, NaCl vs KCl, and pH or 2) concentration, wt%  $CO_3^{2-}$ , and pH

Concentration	Mean	Groups	Groups
0.05	1.46292	A	
0.1	1.18208		В
0.2	1.06708		В
0	1.04909		В

**Table 3.** The average  $\Delta pH$  when considering initial wt%  $CO_3^{2-}$ .

3-way ANOVA comparisons: 1) concentration, wt%  $CO_3^{2-}$ , and pH or 2) wt%  $CO_3^{2-}$ , NaCl vs KCl, and pH

wt% CO <sub>3</sub> <sup>2-</sup>	Mean	Groups	Groups
7	1.49146	A	
3	0.94		В

**Table 4.** The average  $\Delta pH$  when considering NaCl vs KCl.

3-way ANOVA comparisons: 1) wt%  ${\rm CO_3}^{2-}$ , NaCl vs KCl, and pH or 2) Concentration, NaCl vs KCl, and pH

	Mean	Groups	Groups
KCl	1.43333	A	
0	1.04909		В
NaC1	1.04139		В

## % \( \Delta Mass

**Table 5.** The average % $\Delta$ mass when considering NaCl vs KCl for 3 wt% CO<sub>3</sub><sup>2-</sup> apatites.

3-way ANOVA comparison: 1) concentration, NaCl vs KCl, and pH

	Mean	Groups	Groups	Groups
KC1	-14.4212	A		
0	-31.0911		В	
NaC1	-35.7236			С

**Table 6.** The average % $\Delta$ mass when considering NaCl vs KCl for 7 wt% CO<sub>3</sub><sup>2-</sup> apatites.

3-way ANOVA comparison: 1) concentration, NaCl vs KCl, and pH

	Mean	Groups	Groups	Groups
KC1	1.88889	A		
0	-31.6		В	
NaC1	-39.7682			С

**Table 7.** The average  $\%\Delta$ mass when considering KCl groups only.

3-way ANOVA comparison: 1) concentration, wt% CO<sub>3</sub><sup>2-</sup>, and pH

wt% CO <sub>3</sub> <sup>2-</sup>	Mean	Groups	Groups
7	-5.3913	A	
3	-18.0451		В

**Table 8.** The average %∆mass when considering NaCl groups only.

3-way ANOVA comparison: 1) concentration, wt% CO<sub>3</sub><sup>2-</sup>, and pH

wt% CO <sub>3</sub> <sup>2-</sup>	Mean	Groups	Groups
3	-34.7166	A	
7	-37.9925		В

### CO<sub>3</sub>/PO<sub>4</sub>

**Table 9.** The average  $\%\Delta CO3/PO4$  when considering 3 wt%  $CO_3^{2-}$  groups only.

3-way ANOVA comparisons: 1) NaCl vs KCl, concentration, and pH

	Mean	Groups	Groups
KCl	20.65737	A	
0	6.36478		В

NaCl	5.75322		В
------	---------	--	---

**Table 10.** The average %ΔCO3/PO4 when considering NaCl groups only.

3-way ANOVA comparison: 1) wt% CO<sub>3</sub><sup>2-</sup>, concentration, and pH

wt% CO3 <sup>2-</sup>	NaCl	рН	Mean	Groups	Groups	Groups	Groups
	Concentration						
2	0.1	7.4	29.17796	A			
2	0.05	7.4	17.34727	A	В		
2	0.2	7.4	8.47931		В	С	
7	0.2	5.5	4.19577		В	С	D
2	0.05	5.5	-0.51833		В	С	D
7	0.1	5.5	-1.17393		В	С	D
7	0.05	5.5	-3.47968			С	D
7	0.1	7.4	-3.79715			С	D
7	0.2	7.4	-5.18287			С	D
7	0.05	7.4	-5.6996			С	D
2	0.2	5.5	-7.22486			С	D
2	0.1	5.5	-12.742				D

**Table 11.** The average  $\%\Delta CO3/PO4$  when considering KCl groups only.

3-way ANOVA comparison: 1) wt% CO<sub>3</sub><sup>2-</sup>, concentration, and pH

wt% CO <sub>3</sub> <sup>2-</sup>	KC1	pН	Mean	Groups	Groups	Groups	Groups	Groups
	Concentration							
2	0.1	7.4	35.81487	A				
2	0.2	7.4	32.53626	A	В			
2	0.05	7.4	25.62518	A	В			
2	0.2	5.5	25.4579		В			
2	0.1	5.5	7.7603			С		
7	0.2	7.4	6.77031			С	D	
7	0.05	5.5	4.20014			С	D	
7	0.2	5.5	3.79685			C	D	
7	0.05	7.4	1.87884			С	D	Е
2	0.05	5.5	-3.25028				D	Е
7	0.1	5.5	-7.04293					Е
7	0.1	7.4	-7.39904					Е

## Crystallite length and width

**Table 12.** The average crystallite length when considering wt%  $CO_3^{2-}$ .

#### **Supplemental Tables**

3-way ANOVA comparison: 1) wt% CO<sub>3</sub><sup>2-</sup>, pH, and NaCl vs KCl or 2) wt% CO<sub>3</sub><sup>2-</sup>, NaCl vs KCl, and concentration

wt% CO <sub>3</sub> <sup>2-</sup>	Mean	Groups	Groups
3	285.9422	A	
7	145.056		В

**Table 13.** The average crystallite width when considering wt% CO<sub>3</sub><sup>2</sup>.

3-way ANOVA comparison: 1) wt% CO<sub>3</sub><sup>2-</sup>, pH, and NaCl vs KCl or 2) wt% CO<sub>3</sub><sup>2-</sup>, NaCl vs KCl, and concentration

wt% CO <sub>3</sub> <sup>2-</sup>	Mean	Groups	Groups
3	86.33941	A	
7	56.99063		В

Table 14. The average crystallite width when considering NaCl vs KCl.

3-way ANOVA comparison: 1) wt% CO3<sup>2-</sup>, pH, and NaCl vs KCl

Na vs K gro	ouping	crystallite width		
	Mean	Groups	Groups	Groups
NaCl	84.33839	A		
water	75.822		В	
unexposed	65.81383		В	
apatite				
KC1	59.42935			C

**Declaration of Interest** 

**Declaration of interests** 

oxtimes The authors declare that they have no known competing financial interests or personal relationships that could have appeared to influence the work reported in this paper.
□The authors declare the following financial interests/personal relationships which may be considered as potential competing interests: